Fisheries New Zealand
Tini a Tangaroa

Growth of juvenile red rock lobster (*Jasus edwardsii*) in New Zealand and implications for stock assessment

New Zealand Fisheries Assessment Report 2022/45

J. Roberts,
D.N. Webber

ISSN 1179-5352 (online)
ISBN 978-1-99-105228-5 (online)

September 2022

Te Kāwanatanga o Aotearoa
New Zealand Government

Requests for further copies should be directed to:

Fisheries Science Editor
Fisheries New Zealand
Ministry for Primary Industries
PO Box 2526
Wellington 6140
NEW ZEALAND

Email: Fisheries-Science.Editor@mpi.govt.nz
Telephone: 0800 00 83 33

This publication is also available on the Ministry for Primary Industries websites at:
http://www.mpi.govt.nz/news-and-resources/publications
http://fs.fish.govt.nz go to Document library/Research reports

Please cite this report as:

Roberts, J.; Webber, D.N. (2022). Growth of juvenile red rock lobster (*Jasus edwardsii*) in New Zealand and implications for stock assessment. *New Zealand Fisheries Assessment Report 2022/45.* 59 p.

TABLE OF CONTENTS

EXECUTIVE SUMMARY

Roberts, J.[1]; Webber, D.N.[2] (2022). Growth of juvenile red rock lobster (*Jasus edwardsii*) in New Zealand and implications for stock assessment.

***New Zealand Fisheries Assessment Report 2022/45.* 59 p.**

This document describes an analysis of the growth of juvenile (pre-recruit) red rock lobster (*Jasus edwardsii*) around New Zealand. The objectives of this analysis were to: estimate the time lag from puerulus settlement to recruitment, as specified in New Zealand red rock lobster stock assessment models; estimate the size distribution at recruitment; and inform the estimation of growth rate around the size-at-recruitment.

Various sources of juvenile growth information were obtained from previous research, including length and mark-recapture data from wild populations at different locations, and a longitudinal study of captive post-puerulus lobsters. The best growth information came from size composition data collected by diver surveys at Halfmoon Bay, Stewart Island, during the winter months of 1982–2000. Up to four modal groups were apparent from these data, which were informative of the growth rate from 1 to 4 years post-settlement.

A two-step modelling approach was used to estimate growth from the size composition data at Halfmoon Bay: (1) fitting mixture models to the size composition data, and then (2) fitting growth models to the resulting mean sizes of cohorts across multiple years. The optimal model for Halfmoon Bay specified a separate growth curve with respect to size for each sex. This approach was repeated for length-based juvenile growth information from Gisborne Wharf. The predicted growth rates from this model were corroborated by other sources of information, including: mark-recapture growth increment data from juveniles sampled by diver surveys at Stewart Island, and other domestic/overseas growth studies of juvenile red rock lobsters.

The size distribution at 1–4 years post settlement was predicted by a length-based growth model for Halfmoon Bay. This indicated that the timing of recruitment to recent stock assessment models occurs between 2 and 3 years post-settlement. This lag period may vary around New Zealand and is likely to be shorter in CRA 1 and CRA 2 (based on fishery tag data of post-recruits) and in CRA 3 (based on juvenile size-based growth information) relative to the other Quota Management Areas (QMAs).

Based on this analysis, future stock assessments fitting to puerulus indices should only consider time lags from settlement to recruitment of 2 years (approximately 28 mm tail width for both males and females) to 3 years (36 mm and 38 mm tail width for males and females, respectively), with a standard deviation of around 2.5 mm tail width at recruitment when this occurs between 30–35 mm tail width. The annual growth increment at 30 mm tail width is approximately 9 mm tail width based on Stewart Island growth information and around 12 mm tail width based on the analysis of Gisborne Wharf data. Pre-recruitment growth information was lacking for all other regions of New Zealand, although the juvenile growth may be faster still in CRA 1 and CRA 2, based on fishery tag data.

---

[1] Anemone, New Zealand.
[2] Quantifish Limited, New Zealand.

1. INTRODUCTION

1.1 Background

New Zealand red rock lobster (*Jasus edwardsii*) stocks are currently assessed using length-based assessment models that track the number of individuals within a stock across a range of tail width (TW) bins[3]. Growth is estimated within these stock assessment models using mark-recapture data from lobsters recaptured by the commercial and recreational fisheries (e.g., Webber et al. 2020, Rudd et al. 2021a). Some of the assessed stocks have associated puerulus settlement index series (Forman et al. 2020), which aim to monitor changes in the relative rate of puerulus settlement through time. These are long-term time series which have been collected in a standardised way and it is assumed that they are representative of local recruitment strength. For those stocks having these data, stock assessment models have been fitted to these series in the expectation that they will inform recruitment and help with predicting future changes in productivity experienced by the fishery. However, in the past, the stock assessment model fits to the puerulus indices were often poor (e.g., Haist et al. 2015), with the recruitments estimated from the settlement often in conflict with the recruitments estimated by the stock assessment model (which is fitted to data collected from the fishery). The reasons for this conflict are poorly understood.

One possible explanation for this conflict is the uncertain length of time it takes to grow from settlement to the first TW bin used in the stock assessment model. In all recent stock assessment models, growth was modelled based on fishery tag-recapture data, which contain few observations of small lobsters (i.e., less than 40 mm TW) for all New Zealand stocks. Consequently, estimates of growth in the smallest TW bins are highly uncertain and models cannot be expected to extrapolate all the way back to the size at puerulus settlement. In the past, the time lag between settlement and recruitment was derived using puerulus randomisation trials, which fitted randomly re-ordered puerulus settlement index series in the full model using a range of time lags (usually 0, 1, 2, 3, and 4-year lags) and then evaluating the statistical properties of each fit compared to the actual series and selecting the time lag which provided the best overall model fit. However, this approach does not make use of existing juvenile growth information (e.g., McKoy & Esterman 1981, Annala & Bycroft 1985) and often resulted in time lags that lack biological credibility (e.g., 0 or 1 years).

The objectives of this juvenile growth analysis were to:

- estimate the time lag from puerulus settlement to recruitment to the stock assessment model (i.e., 30 mm TW);
- estimate the size distribution and seasonality of recruits to the stock assessment model; and
- inform the estimation of growth rate around the size-at-recruitment to the stock assessment model.

1.2 Methodological approach

Multiple sources of data were used to estimate juvenile growth, including: size composition and mark-recapture data from diver surveys, and a tank-based growth study of captive lobsters. Some of these data have previously been used in published analyses of juvenile growth (e.g., McKoy & Esterman 1981, Annala & Bycroft 1985).

Nearly all of the raw juvenile growth data was reported in terms of carapace length (CL), whereas the length-based stock assessments of New Zealand stocks use TW. Hence, a morphological model was also developed for predicting TW given CL.

Bayesian inference was used to sample from the posterior distribution of all models using the *R* package *brms* (Bürkner 2017, R Core Team 2019) and model selection was guided by the comparison of the leave-one-out information criterion (LOO IC) (Vehtari et al. 2017).

---

[3] The rock lobster stock assessment model tracks numbers of lobsters by TW aggregated into 2 mm size bins. Generally, these bins range from $[30,32),\dots,[90,\infty)$.

2. CONVERTING TO TAIL WIDTH

2.1 Data and methods

Paired CL and TW measurements from juvenile lobsters were obtained from three different sources:

- Measurements from the Gisborne area, digitised from a hand-drawn scatterplot provided by John Booth (unpublished data). These were mostly unsexed apart from some of the larger individuals.
- Halfmoon Bay, Stewart Island, provided in a spreadsheet provided by Paul Breen (unpublished data). These data were all sexed.
- Paired measurements of post-recruits made by the commercial pot fishery data and recorded in the rock lobster catch sampling (*rlcs*) database (Mackay & George 2002).

The selection of data subsets to use for each model was guided by a prior exploration of the raw data. Linear models were fitted to paired CL and TW measurements to allow the prediction of TW given CL. Both CL and TW were log-transformed prior to model fitting such that

Equation 1:

$$\begin{gathered}\log(\mathrm{TW}) \sim \mathrm{N}\left(\mu^{\mathrm{TW}}, \sigma^2\right) \\ \mu^{\mathrm{TW}} = \alpha + \beta \log(\mathrm{CL}) \\ \alpha \sim \mathrm{student}(3, 3.6, 2.5) \\ \sigma \sim \mathrm{student}(3, 0, 2.5)\end{gathered}$$

where α is the slope, β is the intercept, and σ is the standard deviation of the normal distribution. A Student-t distribution was also trialled as a sensitivity to the normal distribution, although this was not found to alter model predictions.

2.2 Results

Based on the CL-TW relationship of juvenile lobsters recorded by historical diver surveys, their morphology does not appear to vary much by sex or region up to 50 mm CL (~30 mm TW) (Figure A.1). At sizes greater than this, females tend to have a greater TW than males (Figure A.1), with very little overlap by sex in individual measurements of TW at around 100 mm CL, based on fishery measurements (Figure A.2). There was also evidence for some regional variability in morphology with increasing CL, with a greater relative TW of females in CRA 2–5 than in CRA 6–8 (insufficient data in CRA 1 and CRA 9) (Figure A.2). There may also be some regional variability in the morphology of males, although the differences appear to be smaller than for females when comparing Quota Management Areas (QMAs) (Figure A.2).

Based on this exploration, it was decided to estimate:

- separate CL-TW relationships for males and females using the diver survey data from Halfmoon Bay; and
- a combined sex CL-TW relationship using the data from Gisborne (nearly all these data were unsexed).

When comparing the CL-TW data for diver surveys with the fishery catch sampling data from the respective statistical areas, the agreement between these data sources was good for Gisborne / statistical area 910, but was not so good for Halfmoon Bay / statistical area 924 (Figure A.3). It was decided to use only the diver survey data for both areas, since these data appeared to be informative across the range of CLs required for converting juvenile growth from CL to TW.

Markov chain Monte Carlo (MCMC) trace plots indicated good mixing for the Halfmoon Bay models for males (model *tw_m*) and females (*tw_f*) (Figure B.1), as well as for the Gisborne model (Figure B.2).

Posterior predictive check plots indicated that the model distributional assumptions were met (Figure B.3 and Figure B.4). The values of all estimated parameters are shown in Table C.1 to Table C.3, and predicted relationships are shown in Figure 1 (Halfmoon Bay) and Figure 2 (Gisborne).

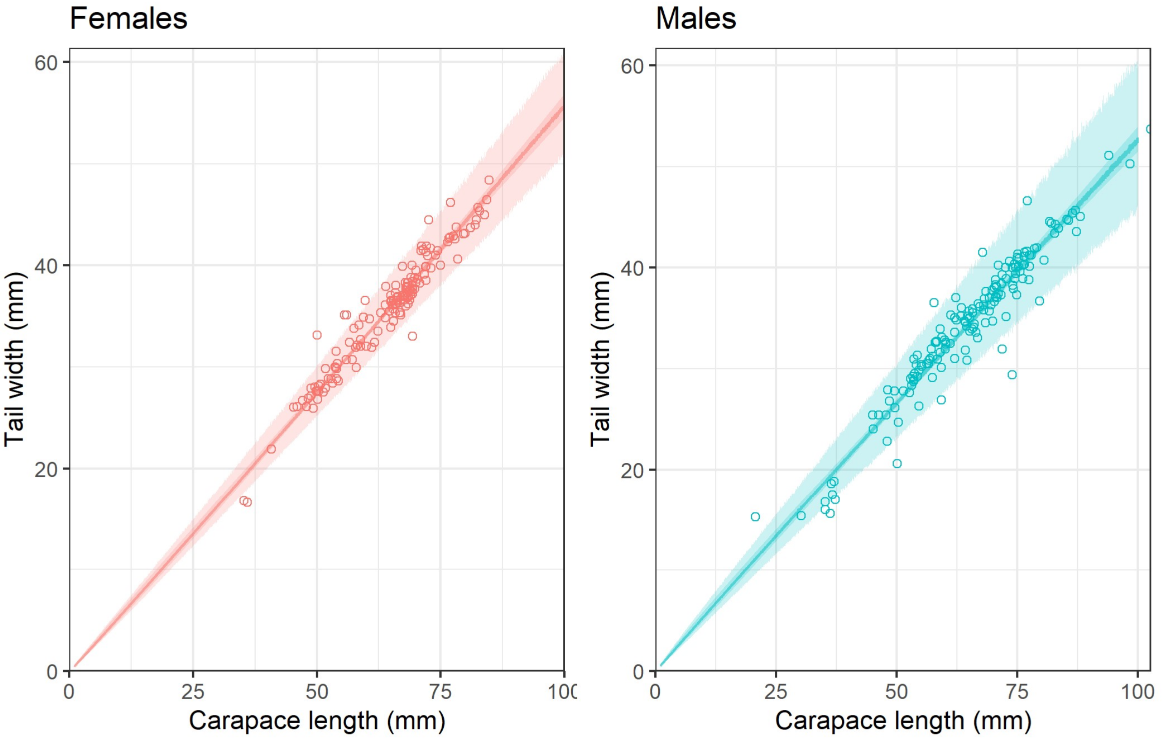

Figure 1: **Paired carapace length (CL) and tail width (TW) measurements of female (left) and male (right) juveniles at <u>Halfmoon Bay, Stewart Island</u> and the predicted relationship from models fitted to these data. The solid line is the mean; the inner shaded region is the 95% credible interval of the posterior distribution; the outer shaded region is the 95% credible interval of the posterior predictive distribution; and open circles are the data.**

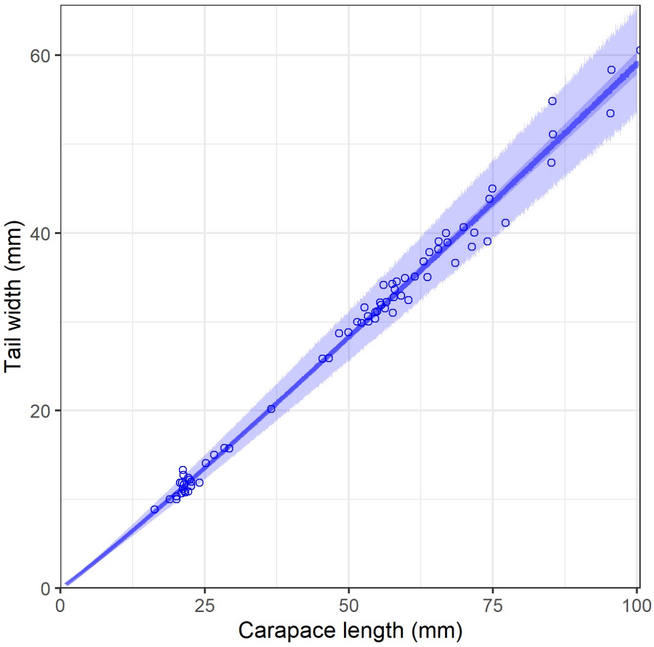

Figure 2: **Paired carapace length (CL) and tail width (TW) measurements of juveniles (combined sex) in the <u>Gisborne region</u> and the predicted relationship from models fitted to these data. The solid line is the mean; the inner shaded region is the 95% credible interval of the posterior distribution; the outer shaded region is the 95% credible interval of the posterior predictive distribution; and open circles are the data.**

3. SIZE-BASED GROWTH

3.1 Data

Multi-year juvenile length frequency (LF) data were obtained from: Halfmoon Bay, Stewart Island (CRA 8) (Paul Breen unpublished data, Jeff Forman unpublished data, *rocklob* database), Gisborne Wharf (CRA 3) (digitised from data plots of McKoy & Esterman 1981), and Wellington Harbour (CRA 4) (*rocklob* database). The sampling protocols used for the collection of these data are described by Annala & Bycroft (1985) (Halfmoon Bay), McKoy & Esterman (1981) (Gisborne Wharf), and Booth et al. (1998) (Wellington Harbour). The timing, size range, and resolution of measurements vary by study:

- Halfmoon Bay, Stewart Island—lobsters sampled each winter (May-August, though June in most years) from 1982 to 2000; sexed LFs were provided to a 1 mm resolution (1982–1997) ranging in size from 21 to 105 mm CL; or to a 5 mm resolution (1998–2000), ranging from 25 to 105 mm CL (Figure A.4 and Figure A.5).
- Gisborne Wharf—lobsters sampled at irregular time intervals from 1976 to 1979 (a total of eight surveys); unsexed LFs provided to a 5 mm resolution, ranging from 20 to 100 mm CL (see McKoy & Esterman 1981) (Figure A.6).
- Wellington Harbour—surveys at multiple sites around Wellington Harbour (see Booth et al. 1998). Samples from Kaiwharawhara were determined through preliminary analytical exploration (not shown here) to have the most promising data for growth estimation, and for which there was at least biannual (summer/winter) sampling of lobsters from 1993 to 1995. These data consisted of unsexed measurements ranging from 30 to 90 mm CL, with a 5 mm resolution (Figure A.7).

3.2 Methods

The growth rate of juvenile red rock lobsters was estimated from the progression of modes present in the length frequency (LF) data. Previous analyses have confirmed a pronounced seasonality of puerulus settlement (peaking in winter at Halfmoon Bay, Gisborne Wharf, and Wellington Harbour) and the presence of discrete cohorts in juvenile size composition data (Booth et al. 1998, Forman et al. 2020).

A two-step approach was taken to estimate daily growth rate from the LF data:

1. fit mixture models to binned LF data to estimate the mean and standard deviation of each mixture component (i.e., each cohort); then
2. fit growth models to the mean size estimates of each cohort, estimate growth rate at size, and derive sizes at *n* years post-settlement.

3.2.1 Mixture models

Mixture models assumed a finite-dimensional mixture modelling approach. The mean of mixture component i was

$$\mu_{i=1,\ldots,K}$$

where K is the number of mixture components (i.e., 1, 2, 3, or 4), and the variance of mixture component i is

$$\sigma^2{}_{i=1,\ldots,K}$$

observation i is

$$x_{i=1,\ldots,K}$$

and the mixture weight for i is

$$\theta_{i=1,\dots,K}$$

which is a simplex of probabilities that sum to one. The probability distribution of an observation is

Equation 2:

$$\begin{gathered}
f(x_i) = \sum_{i=1}^{K} \theta_i \, \mathrm{N}(\mu_i, {\sigma_i}^2) \\
\mu_i \sim \mathrm{student}(3, 60.5, 13.3) \\
\theta_i \sim \mathrm{logistic}(0, 1) \\
\sigma_i \sim \mathrm{student}(3, 0, 13.3)
\end{gathered}$$

where N represents the normal distribution (but any distribution could be used in theory).

Each year/sex combination was modelled independently (i.e., using separate models). For each year/sex combination, three different models were fitted to the Stewart Island LF data (i.e., 1, 2, or 3 mixture components) and four different models were fitted to the Gisborne Wharf LF data (i.e., 1, 2, 3, or 4 mixture components). When running mixture models fitted to these data, it was not possible to reliably estimate the mixture weight (θ) and the standard deviation (SD) of each mixture component (σ) simultaneously. This issue was eliminated when a single SD across all mixture components was assumed for each model run.

The selection of which run to use (i.e., the number of mixture components) was based on the estimated standard error (SE) about the mean of each mixture component (μ). Initial exploration determined that selecting the model with the greatest number of mixture components for which all μ values had SE < 3 resulted in models with an appropriate number of mixture components, given the data. Models with at least one μ SE > 3 typically had at least two posteriors that formed two halves of the same mode. Using a μ SE threshold of 2 resulted in some year/sex combinations which evidently had too few mixture components than were present in the data. Thus, an SE threshold of 3 was determined to be optimal. This method was found to perform better than comparison of the LOO IC for each model, which tended to select models with too many mixture components.

3.2.2 Growth models

The estimates of μ for each mixture component were assigned to a specific age and, therefore, cohort, defined as the year in which they would have settled as pueruli. For Halfmoon Bay, the allocated age was based on the estimated μ of each cohort relative to sex-specific thresholds (Table 1). These thresholds were found to result in no more than one μ in each age and year, for each sex, as would be expected given the strong seasonality in puerulus settlement (peaking in winter months) at Halfmoon Bay (Forman et al. 2020). For Gisborne Wharf and Wellington Harbour, puerulus settlement also peaks in winter months; however LF sampling was at different times, such that simple size thresholds could not easily be used to determine age and cohort. As such, for these locations, age and cohort were determined by visual inspection of the mixture model outputs (i.e., tracking the progression of cohorts though time).

Table 1: Size thresholds used to infer the age of mixture components from mixture models fitted to length frequency (LF) data from Halfmoon Bay, Stewart Island.

Inferred age	Carapace length bounds (mm)	
(years since settlement)	Males	Females
1	< 45	< 45
2	≥ 45 and < 63	≥ 45 and < 60
3	≥ 63 and < 80	≥ 60 and < 75
4	≥ 80	≥ 75

Daily growth rate was then estimated by a generalised linear mixed model (GLMM) that was fitted to the μ for each mixture component (Equation 2). Errors in the response variable were specified as the standard error (SE) of μ obtained for each mixture component. Thus

Equation 3:

$$\mu_i \sim \mathrm{N}\left(\mu^{\mathrm{CL}}, (\sigma + \mathrm{SE})^2\right)$$
$$\mu^{\mathrm{CL}} = \boldsymbol{X\beta} + \boldsymbol{Z\mu} + \sum_{k=1}^{K} f_k(x_k)$$

where μ^{CL} is the expected CL, $\boldsymbol{\beta}$ and $\boldsymbol{\mu}$ are the coefficients at the population-level (analogous to fixed-effects) and group-level (analogous to random-effects) respectively, and $\boldsymbol{X}$ and $\boldsymbol{Z}$ are the corresponding design matrices. The terms $f_k(x_k)$ are smooth functions based on covariates x_k fitted via splines (Wood 2011). The different models tested included different combinations of sex and date as population-level effects, and age and cohort were always treated as a group-level effects.

3.2.3 Annual growth-at-size

Red rock lobster stock assessment models specify a prior for *Galpha*, a model parameter that describes the mean annual growth increment for a specified TW (*alpha*). Recent stock assessments have specified *alpha* to be 30 or 50 mm TW. The size-based growth analyses reported in this section were informative of growth up to ~90 mm CL (~50 mm TW). Hence it was elected to use the optimal growth models and the relevant CL-TW models to predict the annual growth increment at 30 mm and 40 mm TW.

The optimal length-based growth model (Equation 3) was used to predict the mean CL for ages 1–4 at 0.1 intervals (for each date when using the Gisborne Wharf model, since this did not include age). The respective CL-TW model for Halfmoon Bay or Gisborne (Equation 1) was then used to predict TW at each age/date increment, and the age/date at which the TW was closest to 30 or 40 mm TW was identified. The optimal growth model (Equation 3) was then used to obtain the posterior predictive distribution[4] for the size in CL at this respective age (or date for Gisborne), and then at age + 1 (date + 365 for Gisborne). The relevant CL-TW models (Equation 1) (i.e., sex-based models for Halfmoon Bay applied to Halfmoon Bay growth; combined sex model for Gisborne applied to Gisborne Wharf Growth) were then used to convert the CL posteriors for each age into the posterior distribution[5] of TW. The annual growth increment was then obtained by subtracting the predicted TW at age from the TW at age + 1 (or the date equivalent, for Gisborne). The mean, standard deviation, and 95% credible interval (CI) were reported for the resulting annual TW increment at 30 and 40 mm TW.

3.2.4 Predicting size-at-age

The final growth model (Equation 3) that was used to estimate growth rate at Halfmoon Bay from LF data included age (years since settlement as pueruli) as a predictor. In addition to estimating annual growth increments-at-size, this model was used to predict the TW distribution at different ages post-settlement, to determine the probable age at recruitment to stock assessment models. First, the final LF-based Halfmoon Bay growth model was used to obtain the posterior predictive distribution of CL by sex at 1, 2, 3, and 4 years post-settlement. Then, the CL samples were converted to TW by drawing samples from the posterior distribution of the relevant CL-TW model (Equation 1) for each sex. The mean, standard deviation, median, and 95% CI were reported for the resulting TW posteriors.

---

[4] The posterior predictive distribution includes both parameter uncertainty and uncertainty associated with the assumed distribution. The posterior predictive distribution can be sampled from using the *posterior_predict* function in *brms*.

[5] The posterior distribution includes uncertainty in the expected value/mean and can be sampled from using the *posterior_epred* function in *brms*. By definition, these predictions have smaller variance than the posterior predictions performed by the *posterior_predict* method. This is because only the uncertainty in the mean is incorporated in the draws computed by *posterior_epred* while any residual error is ignored. However, the estimated means of both methods averaged across draws should be very similar.

3.3 Results

3.3.1 Halfmoon Bay

The annual size composition data of juvenile red rock lobsters sampled by diver surveys at Halfmoon Bay, Stewart Island, in the winters of 1982–2000, are shown in Figure A.4 and Figure A.5. The raw data were available at different resolutions (1 mm CL for 1982–1997 and 5 mm CL for 1998–2000). A preliminary exploration (not shown here) found that decreasing the resolution from 1 mm CL to 5 mm had a negligible effect on model estimates of growth. Hence, all data were used and related to each other by growth models with some cohorts spanning the two data resolution periods.

MCMC mixing was adequate for all of the final mixture model runs for each year/sex combination (e.g., Figure B.5 to Figure B.7). Reasonably good model fits were obtained to the size composition data (Figure B.8 and Figure B.9).

The median estimates of μ from the final mixture models for each sex/year combination are shown in Figure 3 (arranged by year of measurement and inferred age) and in Figure 4 (arranged by year of measurement and inferred cohort). The size progression (inferred growth) by year was consistent across all cohorts, indicating that the mixture modelling component of the growth estimation from LF data was coherent across all models. Given the optimal mixture models outputs and the CL-based size bands used to infer ages (Table 1), there was not more than one cohort at each age in each year (Figure 3). This is consistent with the strong winter peak in puerulus settlement in winter months, which should result in only one strong size cohort in each year. Estimates of μ were always precise at 2–3 years post-settlement and were reasonably precise for most estimates at 1 and 4 years.

Seven alternative model structures were compared for estimating juvenile growth rate when fitting to the mixture model outputs (Table 2). Three simple models did not estimate growth and were only for comparison: the null model (*lf_hm_1*), which simply estimated an overall mean size; a variation to this that included a random intercept for cohort (*lf_hm_2*); and another that included this as well as sex (*lf_hm_3*). Two growth models estimated size relative to measurement date: one model that included date and a cohort random effect (*lf_hm_4*), and another that also allowed the date effect to vary by sex (*lf_hm_5*). Two growth models estimated size relative to the inferred age of each cohort at the date of measurement: one that estimated a curvilinear response of size-at-age, using a separate spline for each sex (*lf_hm_6*); and another that also included a random intercept for cohort (*lf_hm_7*). Models that did not include growth were much less parsimonious than models that did (Table 2).

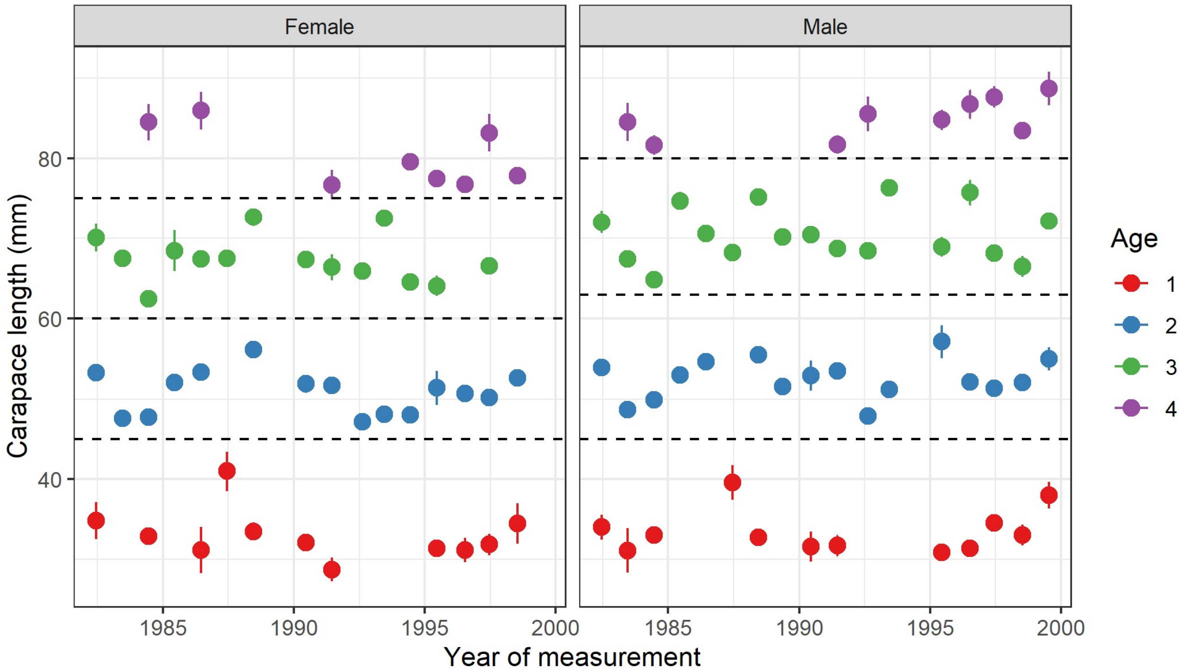

Figure 3: The mean carapace length (CL, points) of juvenile lobsters by year and sex predicted from mixture models fitted to diver sampling length frequencies (LFs) at Halfmoon Bay, Stewart Island during 1982–2000. Whiskers represent the standard deviation associated with estimated mean values. Cohort ages (from 1 to 4 years post-settlement) were inferred based on sex-specific size bands (Table 1), which are represented here as horizontal lines. Data gaps occurred where optimal mixture models for a year/sex combination had less than four components, or where no optimal model was obtained.

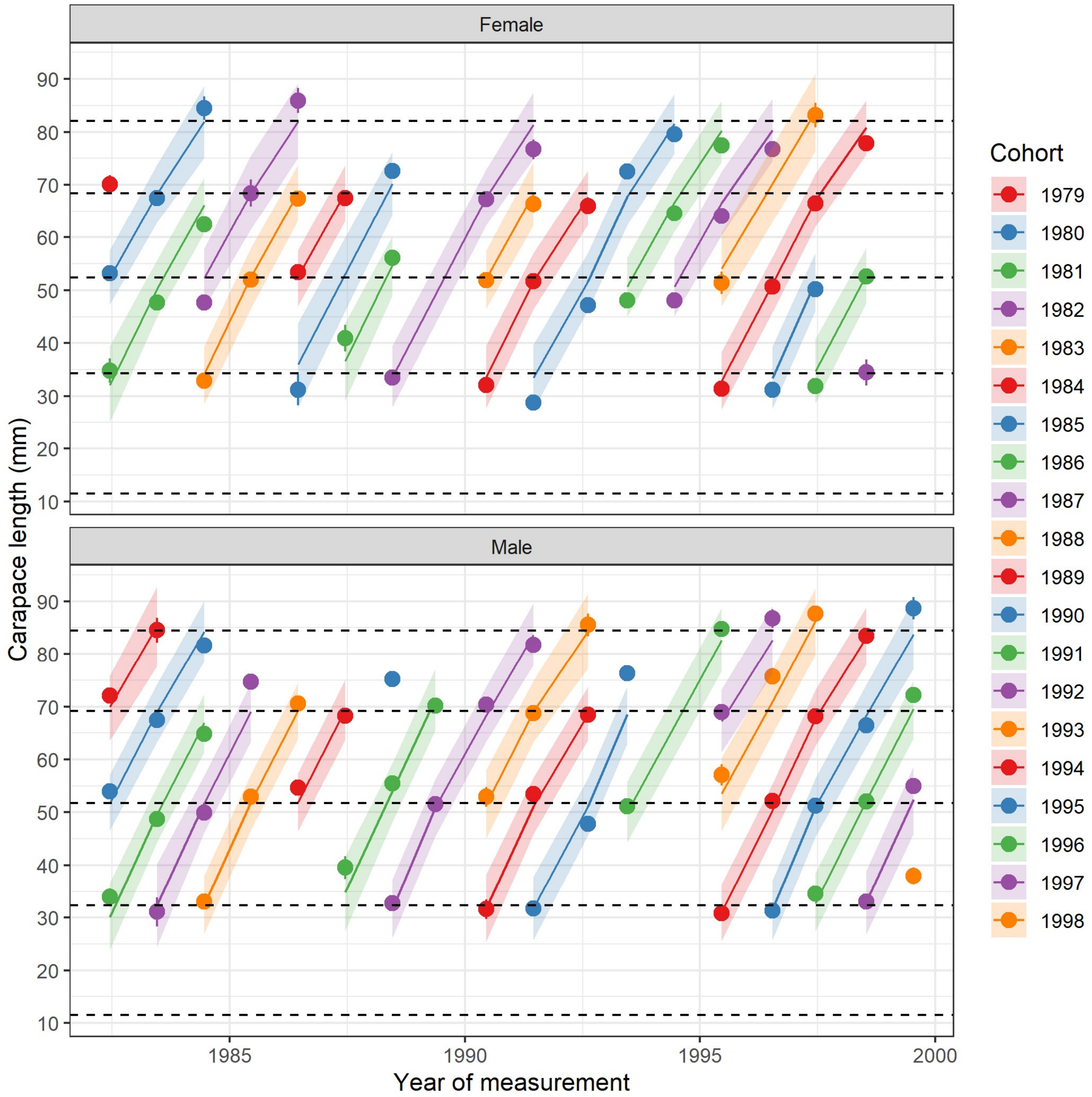

Figure 4: Growth model fit (model *lf_hm_7* from Table 2) to mixture model estimates of the size-at-age of lobsters sampled by diver surveys at Halfmoon Bay, Stewart Island during 1982–2000. Solid lines and shaded areas represent the mean and 95% credible intervals predicted by the growth model. Points and whiskers represent the estimated mean and associated standard deviation of the mean size-at-age of each cohort predicted by mixture models fitted to length-frequency data. The horizontal dashed lines represent the mean estimated carapace length across all cohorts at 1–4 years post-settlement, with the exception of the bottom line, which represents the mean size of pueruli (11.5 mm carapace length), reported by Booth (1979).

Table 2: Comparison of models for estimating the growth rate of juvenile red rock lobsters using length-frequency (LF) data from Halfmoon Bay, Stewart Island. LOO IC = leave-one-out information criterion. The optimal growth model used for inference is in bold. 's(age, by = sex, k = 3)' specifies a sex-specific spline of size with respect to age; '1|cohort' specifies a random intercept for each cohort (allowing cohorts to have a different carapace length at each age, but not allowing growth rate to vary by cohort).

ID	Model structure	Model type	LOO IC	δ-LOO IC	SE LOO IC
lf_hm_7	**mu|se ~ s(age, by = sex, k = 3) + (1|cohort)**	**Age**	**517.3**	**0.0**	**15.6**
lf_hm_6	mu|se ~ s(age, by = sex, k = 3)	Age	529.0	11.7	13.3
lf_hm_5	mu|se ~ sex:date + (1|cohort)	Date	534.7	17.4	17.7
lf_hm_4	mu|se ~ date + (1|cohort)	Date	550.5	33.2	18.6
lf_hm_1	mu|se ~ 1	No growth	874.2	356.9	9.6
lf_hm_2	mu|se ~ 1 + (1|cohort)	No growth	875.4	358.1	9.5
lf_hm_1	mu|se ~ sex + (1|cohort)	No growth	876.7	359.4	9.6

The model estimating a sex-specific size-at-age with a cohort random effect (*lf_hm_7*) was the best model in terms of LOO IC and was used for making inference. Expanding on Equation 3, this model was

Equation 4:

$$\begin{gathered}\mu^{\mathrm{CL}} = \beta_0 + Z_h\mu_h + f_{s,a}\left(x_{s,a}\right) \\ \beta_0 \sim \mathrm{student}(3, 55.2, 21.6) \\ \mu_h \sim \mathrm{N}\left(0, \left(\sigma^h\right)^2\right) \\ \sigma^h \sim \mathrm{student}(3, 0, 21.6) \\ \sigma \sim \mathrm{student}(3, 0, 21.6)\end{gathered}$$

where β_0 is the intercept, μ_h is the group level effect for each cohort (h), $f_{s,a}\left(x_{s,a}\right)$ is a spline over ages (a) for each sex (s), and σ is the standard deviation of the normal distribution.

MCMC mixing for this model was good for all estimated parameters (Figure B.10), and the density of predictions agreed well with the observations, across the full range of carapace lengths (Figure B.11).

Based on predictions from the optimal growth model fitted to size-based information from Halfmoon Bay:

- 30 mm TW was attained at around age 2.2 for males (29.5 mm TW) and females (30.8 mm TW); and
- 40 mm TW was attained at around age 3.4 for males (39.8 mm TW) and females (41.0 mm TW).

The predicted annual growth increments at 30 mm TW and 40 mm TW are shown in Table 3 and Figure 5. A slightly faster growth increment was estimated for males at both sizes, which was slightly slower for both sexes at 40 mm TW (e.g., a mean of 7.51 mm TW for females) than at 30 mm TW (a mean of 8.68 mm TW for females). Comparable estimates of annual growth at 30 mm TW were estimated from the optimal linear model (*lf_hm_5*): 8.54 mm TW for males (95% CI = 4.47–12.82) and 9.12 mm TW for females (95% CI = 4.82–13.69), noting that these estimates integrate growth information across the period 1–4 years post-settlement.

Table 3: Predicted annual tail-width increment of lobsters at 30 mm tail width and 40 mm tail width, predicted from a model fitted to size-based growth information from Halfmoon Bay, Stewart Island (*lf_hm_7*).

Starting size (mm tail width)	Predicted annual tail-width increment males (mm tail width)					Predicted annual tail-width increment females (mm tail width)				
	Mean	SD	2.5%	Median	97.5%	Mean	SD	2.5%	Median	97.5%
30	8.86	1.95	0.90	8.86	12.68	8.68	2.11	4.39	8.69	12.69
40	7.79	2.13	3.55	7.83	12.01	7.51	2.44	2.52	7.53	12.30

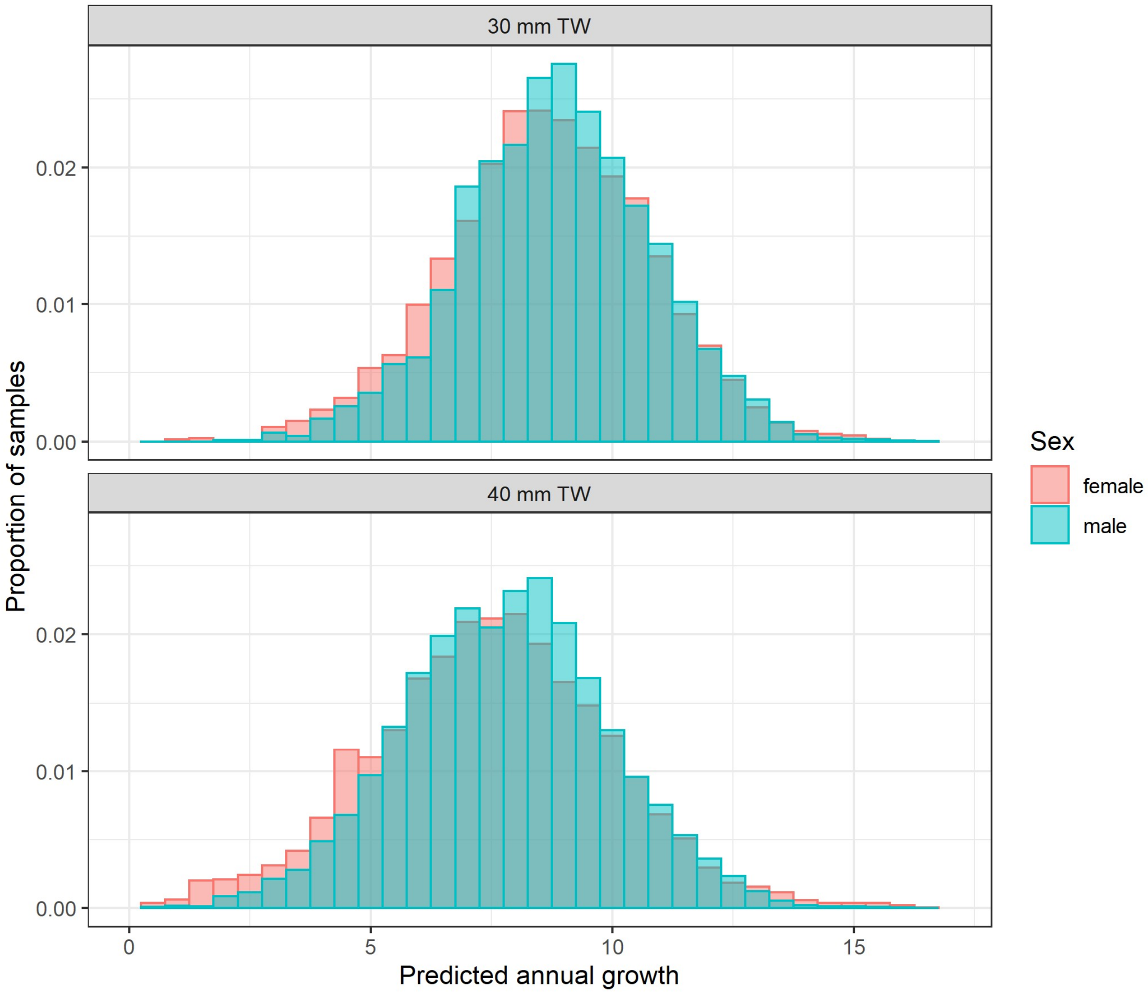

Figure 5: Predicted annual tail-width increment at 30 mm tail width (top) and 40 mm tail width (bottom) of juvenile lobsters by sex at Halfmoon Bay, Stewart Island, predicted from a growth model (*lf_hm_7*) fitted to LF data.

Table 2 and Figure 6 show the predicted TW of lobsters at each age from 1 to 4 years since settlement, using the LF-based growth model for Halfmoon Bay. Based on this model, the time lag from settlement to recruitment in recent stock assessment models (i.e., a mean of 33.35 mm TW) would be approximately 2.5 years. Note that this mean size of recruitment was based on the size at 3 years post-settlement, as estimated by an earlier iteration of this analysis (Webber et al. 2020), which was prior to any formal analysis of the CL-TW relationship.

Due to the way that the TW posteriors were predicted, their shape should approximate the true variability in the size of each cohort at age. The variability in the predicted size distributions varied with age

(Table 2), although σ = 2.5 mm TW would be a valid universal assumption for the size-at-recruitment to stock assessment models, where this occurs at 2–3 years post-settlement.

Table 2: Predicted tail-width (TW) distribution at age (years post-settlement as pueruli) of red rock lobsters at Halfmoon Bay, Stewart Island by sex, predicted from the optimal growth model using length-based information (*lf_hm_7*).

	Predicted tail-width males					Predicted tail-width females				
Age	Mean	SD	2.5%	Median	97.5%	Mean	SD	2.5%	Median	97.5%
1	17.33	1.89	13.79	17.30	21.23	18.54	1.85	15.12	18.51	22.36
2	27.68	2.36	23.46	27.58	32.46	28.84	1.96	25.19	28.77	32.78
3	36.25	2.99	30.60	36.11	42.41	38.09	2.25	33.71	38.08	42.44
4	44.27	3.38	37.97	44.20	51.38	46.06	2.80	40.63	46.05	51.56

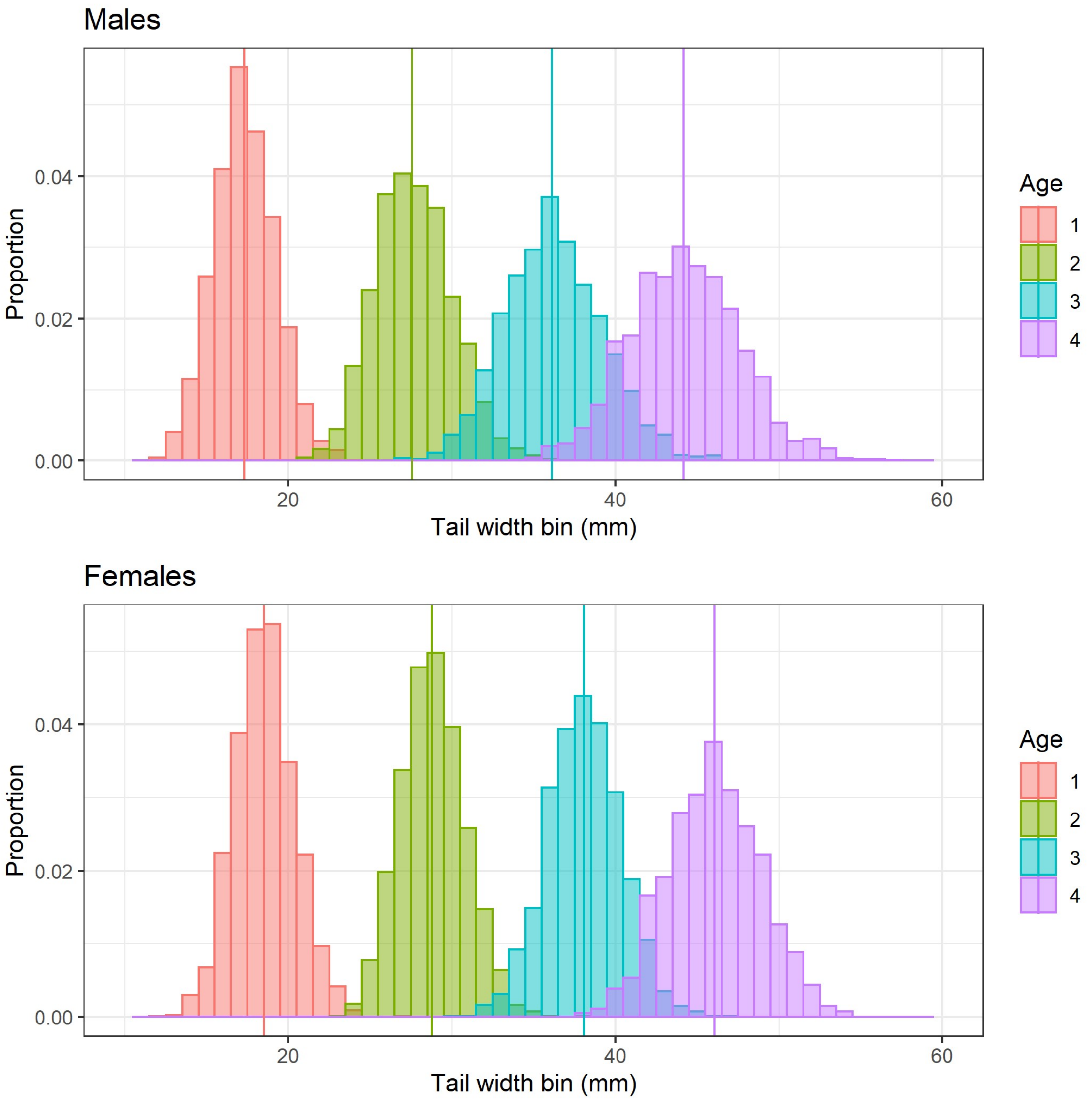

Figure 6: Predicted tail-width (TW) distribution at age (years post-settlement as pueruli) of red rock lobsters at Halfmoon Bay, Stewart Island by sex, predicted from a growth model (*lf_hm_7*) using size-based growth information. Vertical lines represent the median TW at each age.

3.3.2 Gisborne Wharf

The diver survey LF observations from Gisborne Wharf are shown in Figure A.6. MCMC chains indicated good mixing for all of the final mixture model runs for each sampling month (e.g., Figure B.13 to Figure B.15). Reasonably good model fits were obtained to the size composition data (Figure B.16). A summary of model parameter estimates is given in Table C.7.

The median estimates of μ from the final mixture models for each sex/year combination are shown in Figure 7, arranged by year of measurement and putative cohort. Estimates of μ were precise for all mixture components. The size progression (inferred growth) by year was consistent for some cohorts, but not all (i.e., cohort 1 had a relatively fast progression and cohort 5 had a slow progression). All mixture components for each putative cohort were used for subsequent growth estimation.

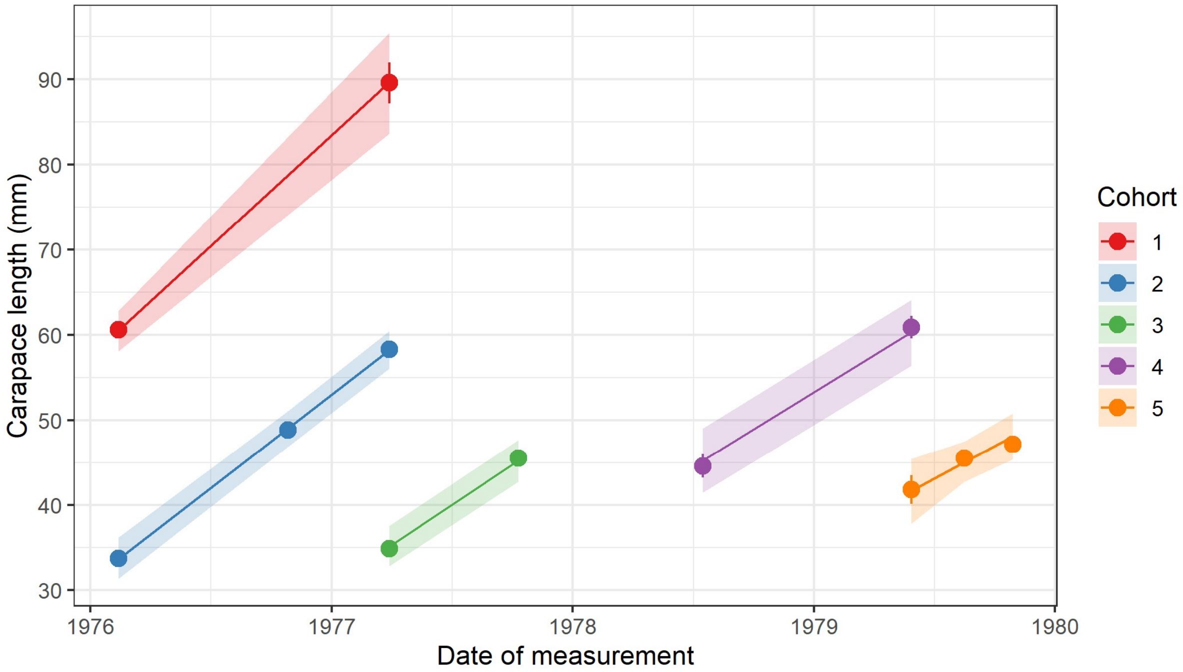

Figure 7: Growth model fit (model *lf_gw_4* from Table 4) to mixture model estimates of the size-at-age of lobsters sampled by diver surveys at Gisborne Wharf during 1976–1979. Solid lines and shaded areas represent the mean and 95% credible intervals predicted by the growth model. Points and whiskers represent the estimated mean and associated standard deviation of the mean size-at-age of each cohort predicted by mixture models fitted to length-frequency data.

Four different model structures were compared for estimating growth rate at Gisborne Wharf (Table 5): the null model (*lf_gw_1*), which simply estimated an overall mean size; the simplest growth model, which only included date (*lf_gw_2*); another that also included a random intercept for cohort (*lf_gw_2*); and, finally, the most complex growth model, which also included a random slope and intercept for cohort (*lf_gw_4*).

The most complex model, estimating a cohort-specific intercept as well as slope with respect to growth rate (*lf_gw_4*), was the best model in terms of LOO IC and was used for making inference. The MCMC run for this model had good mixing for all estimated parameters (Figure B.17), the density of model predictions agreed well with the observations across the full range of sizes (Figure B.11), and the model fits were good (Figure 7). The estimated model parameters are summarised in Table C.7.

Table 5: Comparison of models for estimating the growth rate of juvenile red rock lobsters using length-frequency data from Gisborne Wharf. LOO IC = leave-one-out information criterion. The optimal growth model used for inference is in bold. 'date|cohort' specifies a random slope with respect to the size at date for each cohort (allowing each cohort to have a different growth rate); '1|cohort' simply specifies a random intercept for each cohort (allowing each cohort to have a different size with respect to date, but not a different growth rate).

ID	Model structure	Model type	LOO IC	δ-LOO IC	SE LOO IC
lf_gw_4	**mu|se** ~ date + (date|cohort)	**Date**	**38.9**	**0.0**	**2.4**
lf_gw_3	mu|se ~ date + (1|cohort)	Date	54.9	16.0	4.9
lf_gw_1	mu|se ~ date	Date	103.6	64.7	10.1
lf_gw_2	mu|se ~ 1	No growth	105.0	66.1	8.8

The model estimating a sex-specific size-at-age with a cohort random effect (*lf_gw_4*) was the best model in terms of LOO IC and was used for making inference. Expanding on Equation 3, this model was

Equation 5:

$$\begin{gathered}
\mu^{\mathrm{CL}} = \beta_0 + X_d\beta_d + Z_{d,h}\mu_{d,h} \\
\beta_0 \sim \mathrm{student}(3, 46.4, 11.9) \\
\beta_d \sim \mathrm{N}\left(0, \left(\sigma^d\right)^2\right) \\
\sigma^d \sim \mathrm{student}(3, 0, 11.9) \\
\mu_{d,h} \sim \mathrm{N}\left(0, \left(\sigma^{d,h}\right)^2\right) \\
\sigma^{d,h} \sim \mathrm{student}(3, 0, 11.9) \\
\sigma \sim \mathrm{student}(3, 0, 11.9)
\end{gathered}$$

where β_0 is the intercept, β_d is the population level coefficient for date, $\mu_{d,h}$ is the group level effect for each date and cohort (h), and σ is the standard deviation of the normal distribution.

Because the optimal growth model did not include age, the corresponding date at which 30 mm TW was attained by a chosen cohort was searched for (the 1982 cohort was chosen, although there was no basis for choosing one over another). For cohort 3 (coloured green in Figure 7), 30 mm TW was attained on 2 February 1978 and 40 mm TW was attained on 12 December 1978.

The predicted annual growth increments at 30 mm TW and 40 mm TW are shown in Table 3 and Figure 8. The mean annual growth rate at Gisborne Wharf (e.g., 11.66 mm tail width at a starting size of 30 mm TW; 95% CI = 8.71–14.65) was faster than was predicted for Halfmoon Bay, using the same method (compare with Table 3). Note that, since the growth model was linear, any differences in the predicted growth increment posteriors at 30 mm TW versus 40 mm TW would be driven by curvature and uncertainty in the CL-TW relationship.

Table 3: Predicted annual tail-width (TW) increment of lobsters at 30 mm tail width and 40 mm tail width, predicted from a model fitted to size-based growth information from Gisborne Wharf (*lf_gw_4*).

Starting size	Predicted annual length increment (mm tail width)				
(mm tail width)	Mean	SD	2.5%	Median	97.5%
30	11.66	1.54	8.71	11.66	14.65
40	11.77	1.55	8.71	11.80	14.79

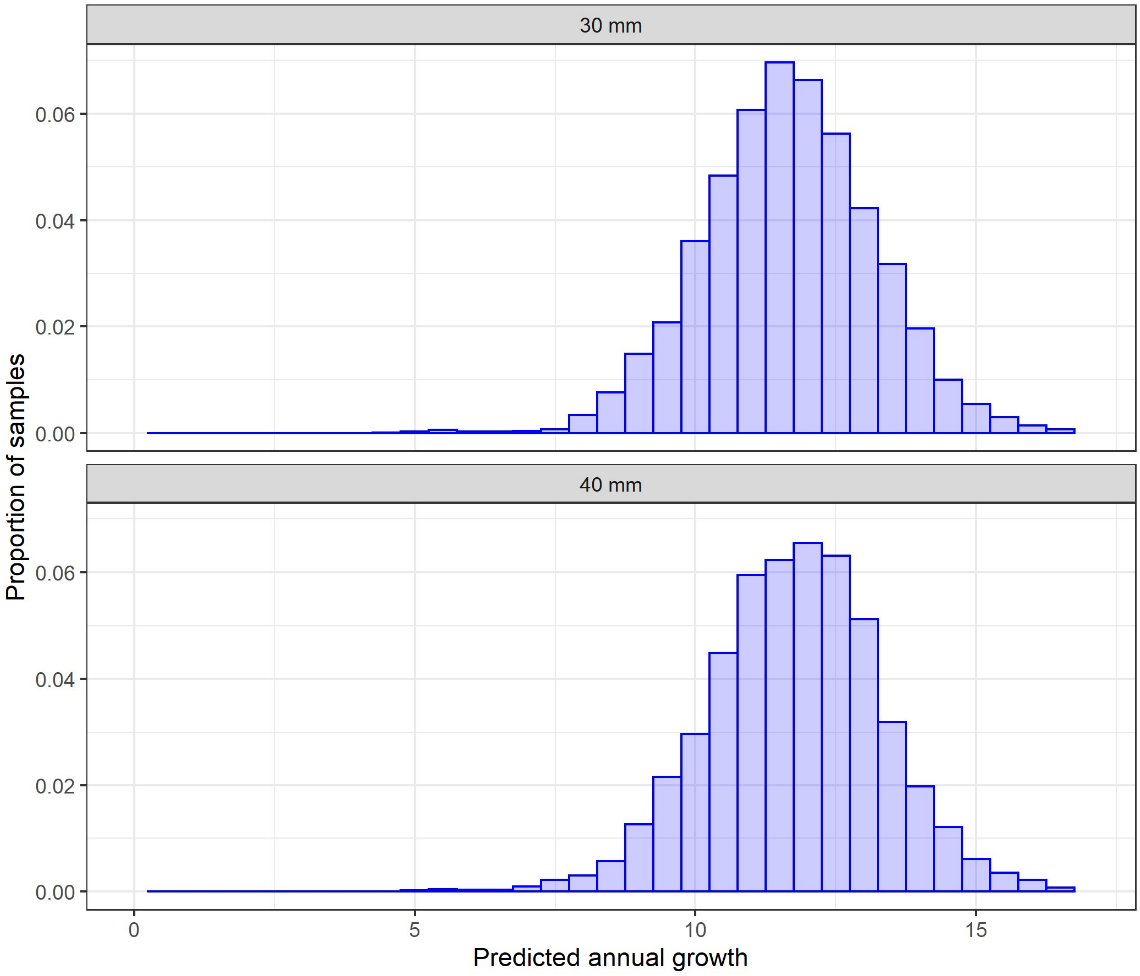

Figure 8: Predicted annual tail-width increment at 30 mm tail width (top) and 40 mm tail width (bottom) of juvenile lobsters at Gisborne Wharf, predicted from a growth model (*lf_gw_4*) fitted to LF data.

Since there was no simple means of estimating age using the Gisborne Wharf data, no attempt was made to estimate the size-at-age from the Gisborne Wharf data. However, based on the faster growth of juveniles estimated here (relative to Halfmoon Bay, above), it is likely that recruitment to stock assessment models (at 30–35 mm TW) would occur closer to two than three years post-settlement.

3.3.3 Wellington Harbour

No more than two cohorts were apparent from a visual inspection of the size composition data from Kaiwharawhara, Wellington Harbour (Figure A.7), and there was little evidence of any predictable progression in the size of these cohorts that could be used to estimate growth. As such, it was decided that these data did not contain sufficient information for estimating growth rate.

4. JUVENILE MARK-BASED GROWTH

4.1 Data and methods

See Appendix A for a brief summary of the survey methods used for collecting juvenile mark-recapture data (Annala & Bycroft 1985 give a fuller description).

Candidate linear and non-linear growth models were fitted to the processed mark-recapture observations, following the modelling approach that was adopted for estimating growth rate from the outputs of mixture models fitted to LF data (see Section 0 for equations). Models were fitted to observed individual lobster size increments, using the midpoints of respective 5 mm CL increment size classes reported by Annala & Bycroft (1985). These midpoints were transformed by dividing by a factor of 5 (e.g., a 5 mm CL increment was modelled as a 1 mm CL increment), so that Poisson and negative binomial error structures could be explored. Candidate model terms included: sex, CL at release (linear or spline), and years spent at liberty (linear or spline). Alternative error structures were also explored (Table 4). The general form for this model was

Equation 6:

$$\frac{\Delta\mathrm{CL}}{5} \sim \mathrm{Poisson}(\lambda^{\Delta\mathrm{CL}})$$

$$\lambda^{\Delta\mathrm{CL}} = \boldsymbol{X\beta} + \boldsymbol{Z\mu} + \sum_{k=1}^{K} f_k(x_k)$$

where $\lambda^{\Delta\mathrm{CL}}$ is the expected CL increment, $\boldsymbol{\beta}$ and $\boldsymbol{\mu}$ are the coefficients at the population-level and group-level respectively, and $\boldsymbol{X}$ and $\boldsymbol{Z}$ are the corresponding design matrices. The terms $f_k(x_k)$ are smooth functions based on covariates x_k fitted via splines (Wood 2011).

Samples from the posterior distribution of the annual growth increment (in mm CL) at 1 year at liberty were obtained. To convert this to a TW-based growth increment, the initial size at release and the size at recapture (both mm CL) samples from the posterior predictive distribution were drawn from models *tw_m* for males and *tw_f* for females (see Section 2). The size increment in TW was then calculated as the difference between the predicted TWs at release and at recapture one year later.

4.2 Results

A preliminary exploration of the mark-recapture size increment data digitised from Annala & Bycroft (1985) found that the growth rate was likely to be biased low when using growth increments obtained from < 1 year at liberty (Figure 9), which may relate to these individuals not completing their annual moult cycle.

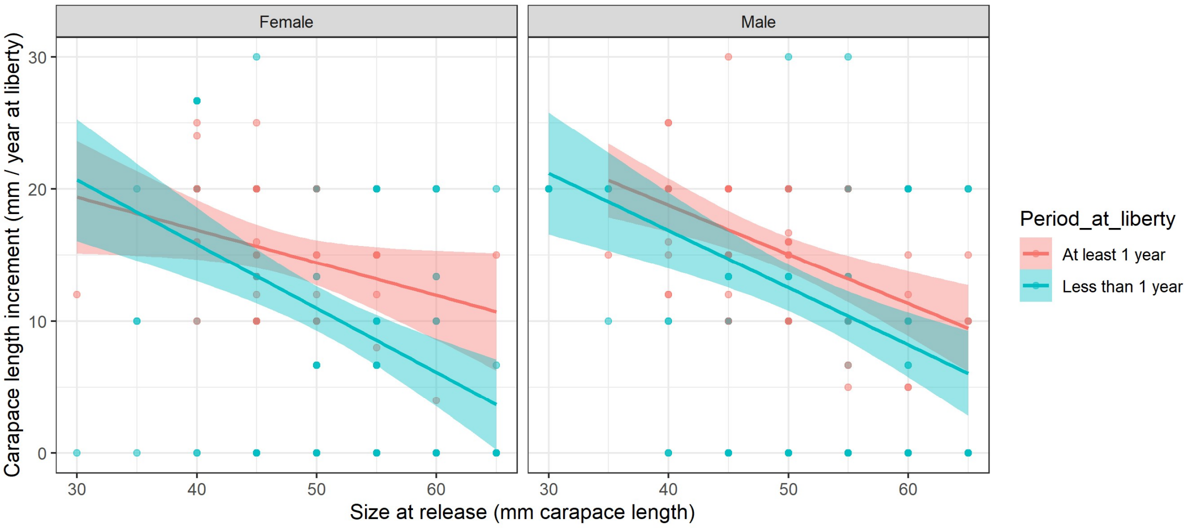

Figure 9: Annualised growth increment of juvenile red rock lobster from a diver-based mark-recapture study at Halfmoon Bay, Stewart Island (data digitised from Annala & Bycroft 1985). The lines represent mean increments, shaded areas represent 95% confidence intervals, and points represent raw data points.

Good MCMC mixing was obtained for all model runs based on the visual inspection of trace plots (Figure B.19).

All models exploring model structure assumed a Poisson distribution. Other distributions were trialled (zero-inflated Poisson, negative binomial, and zero-inflated negative binomial), although the Poisson was preferred based on LOO IC (comparing *tag9*, *tag10*, *tag11*, and *tag12*). Posterior predictive check plots indicated that the Poisson distribution assumptions were approximately met (Figure B.20).

The period spent at liberty was found to the best single model term, based on LOO IC, and using a spline for this term was found to be optimal (model *tag6*). Size at release (also modelled using a spline) was the next best model term. The optimal model structure according to the LOO IC included only these two terms (both modelled using splines) (*tag7*), although the model also including sex (*tag9*) was marginally inferior and was ultimately selected for making predictions, given probable sex-based differences in growth rate from the length-frequency based growth analysis (see Section 3). Parameter estimates for model *tag9* are shown in Table C.9. The conditional smooth plots for model *tag9* are consistent with a decrease in growth rate with increasing size at release and an increase in growth rate with increasing time spent at liberty up to 1 year at liberty, with a plateau from 1 to 1.5 years at liberty (Figure B.21).

Table 4: Comparison of models for estimating the growth rate of juvenile red rock lobsters using mark-recapture data from Halfmoon Bay, Stewart Island. LOO IC = leave-one-out information criterion. The model in bold (*tag9*) was used for making predictions. Model terms are: 'inc' = observed size increment in mm CL; 'yrs_lib' = years individual was spent at liberty; 'cl_rel' = size in mm CL at the time of release, 'sex' = male or female.

ID	Model structure	Distribution	LOO IC	δ-LOO IC	SE LOO IC
tag7	inc/5 ~ s(yrs_lib, k = 3) + s(cl_rel, k = 3)	Poisson	930.2	0	22.1
tag9	**inc/5 ~ s(yrs_lib, k = 3) + s(cl_rel, k = 3) + sex**	**Poisson**	**930.3**	**0.1**	**22.1**
tag10	inc/5 ~ s(yrs_lib, k = 3) + s(cl_rel, k = 3) + sex	Zero-inflated Poisson	932.3	2.1	22.1
tag11	inc/5 ~ s(yrs_lib, k = 3) + s(cl_rel, k = 3) + sex	Negative binomial	933.6	3.4	22.2
tag12	inc/5 ~ s(yrs_lib, k = 3) + s(cl_rel, k = 3) + sex	Zero-inflated negative binomial	935.5	5.3	22.2
tag6	inc/5 ~ s(yrs_lib, k = 3)	Poisson	960.6	30.4	23.1
tag8	inc/5 ~ s(yrs_lib, k = 3) + sex	Poisson	961.5	31.3	23.2
tag5	inc/5 ~ yrs_lib	Poisson	989.3	59.1	23.5
tag4	inc/5 ~ s(cl_rel, k = 3)	Poisson	1186.1	255.9	27.5
tag3	inc/5 ~ cl_rel	Poisson	1195.7	265.5	27.5
tag1	inc/5 ~ 1	Poisson	1275.8	345.6	29.8
tag2	inc/5 ~ sex	Poisson	1277.5	347.3	30.1

The annual growth increment in terms of mm CL was slightly faster for males than for females (although with considerable overlap in 95% CIs). However, when predicted sex-differences in the CL-TW relationship were accounted for, the average growth at size was almost the same for each sex. Growth rates were predicted to decline with increasing size at release, with a median of around 12.5 mm TW annually at 15–20 mm TW, declining to around 7.5 mm TW annually by 30 mm TW, for both sexes (Figure 10).

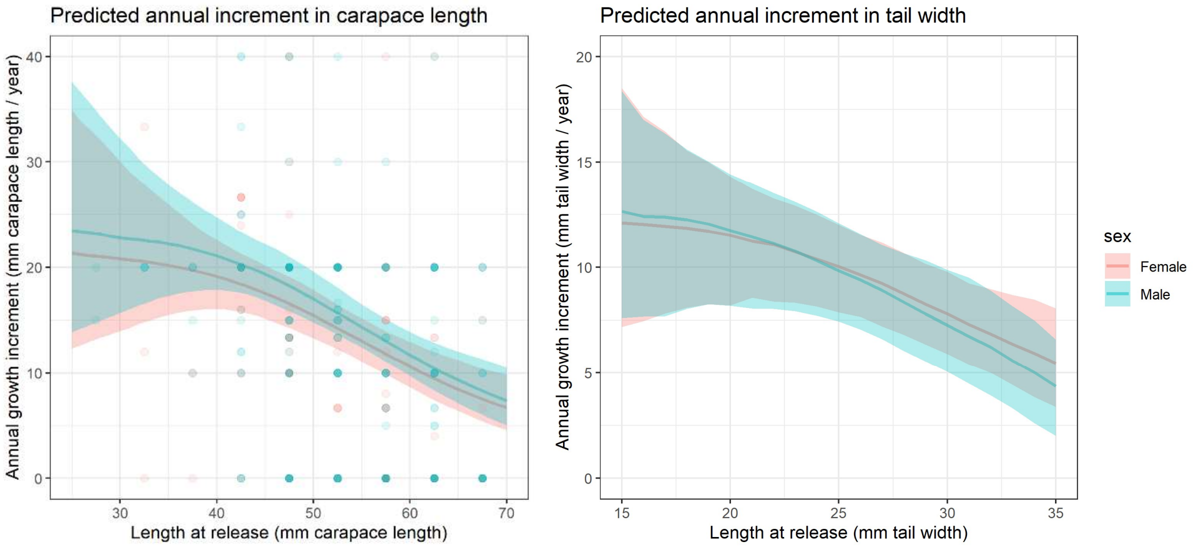

Figure 10: Predicted (using model *tag9*) annual size increment of juvenile males and females by size at release, based on mark-recapture collected by diver surveys at Halfmoon Bay, Stewart Island (Annala & Bycroft 1985), for carapace length (left) and tail width (right). Lines represent the median values and ribbons represent the 95% credible intervals. Annualised raw growth increment data are included and displayed in the carapace length plot.

5. FISHERY TAG-BASED GROWTH

5.1 Observations and methods

A brief analysis of regional variation in growth rate around the size at recruitment was also completed using tag-recapture growth increment records from the commercial pot fishery (retrieved from the *tag* database) (Table A.1). Annualised growth rate was first calculated for each recapture event, based on the reported growth increment (in mm TW) divided by the number of days at liberty (giving δ-TW yr^{-1}). Linear models (using *ggplot2*) (Wickham 2017) were then used to visually assess for potential between-QMA variability in the growth rate given size at release. Note that this presentation of the data does not account for potential temporal variation in growth rate, which could affect growth in each QMA differentially.

5.2 Results

The exploration of the commercial fishery tag data found that relative growth rate of small lobsters (< 50 mm TW at the time of release) was likely to be faster in CRA 1 and CRA 2 than the other QMAs, and this was true for both sexes (Figure A.8). Linear models fitted to these data were best informed for males, for which two discrete growth groups were apparent: CRA 1–2 and CRA 3–8. This was consistent with increased growth rate in the two warmest QMAs and minimal variability across the remaining QMAs.

6. CAPTIVE LOBSTER GROWTH

6.1 Observations and methods

Data were also obtained from a longitudinal growth study of post-puerulus lobsters held captive in tanks at NIWA, Mahanga Bay, Wellington (Graeme Moss unpublished data). Lobsters were given a replete diet of mussels and bathed in seawater at ambient Wellington Harbour temperature. A total of 60 lobsters, ranging from 11 to 19 mm CL at the start of the experiment, were tracked over a period of 211 days. All surviving lobsters were measured at 29, 58, 98, 127, 162, 189, and 211 days over the course of the experiment. It was hypothesised that the growth of these lobsters would represent an approximate upper bound for growth rate in the Wellington region (and colder regions, e.g., Stewart Island) during the first year after settlement as pueruli.

Linear mixed-effects models were fitted to repeated measurements of individual lobsters in the experiment. Alternative model structures were trialled with the general form

Equation 7:

$$\begin{gathered} \mathrm{CL} \sim \mathrm{N}\left(\eta^{\mathrm{CL}}, \sigma^2\right) \\ \eta^{\mathrm{CL}} = \boldsymbol{X\beta} + \boldsymbol{Z\mu} \\ \sigma \sim \mathrm{student}(3, 0, 5.4) \end{gathered}$$

where η^{CL} is the expected CL, $\boldsymbol{\beta}$ and $\boldsymbol{\mu}$ are the coefficients at the population-level and group-level, $\boldsymbol{X}$ and $\boldsymbol{Z}$ are the corresponding design matrices, and σ is the standard deviation of the normal distribution.

6.2 Results

Of the 60 lobsters monitored by this experiment, seven died by the time of the second measurement on the 58th day and were excluded from this analysis, leaving a sample of 53 lobsters. The progression of individual size with each measurement is shown in Figure A.9. Growth was approximately linear for all individuals, although growth rate varied by individual.

Three alternative linear growth model structures were trialled (*mah2*, *mah3*, and *mah4*), all of which specified a day effect on carapace length (Table 8). This was compared with the null model (*mah1*). All models had good MCMC mixing, based on a visual inspection of trace plots (e.g., Figure B.22).

The model specifying a random slope and intercept for individual lobsters (*mah4*) was superior to the others based on LOO IC (Table 8), but it had a less than optimal fit to the data (Figure B.23). Building on Equation 7, this model was

Equation 8:

$$\eta^{\mathrm{CL}} = \beta_0 + X_d\beta_d + Z_{d,i}\mu_{d,i}$$

where β_0 is the intercept, β_d is the slope of the linear ‘day’ population level effect, and $\mu_{d,i}$ is the random slope for day and individual lobster (i). This model predicted a mean annual growth rate of 20.9 mm CL yr^{-1} (95% CI = 19.8–21.9 mm CL yr^{-1}).

In addition, a non-linear growth model (*mah5*) was trialled that was a modification of *mah4* that specified a spline over day (d). This model far out-performed the best linear model in terms of LOO IC (Table 8) and had a much better fit to the data (Figure B.24). The conditional smooth plots for model *mah5* are consistent with an increase in growth rate over the 200-day period of the study (Figure B.25). Although this model was better fitting than the best linear model, the non-linear structure was problematic for making predictions across a whole year, particularly given the 200-day period of the study. However, this model does indicate that the growth rate of lobsters can be faster than the predicted annual increment from *mah4*.

Table 8: Comparison of models for estimating the growth rate of captive post-puerulus red rock lobsters, at NIWA, Mahanga Bay, Wellington (Graeme Moss unpublished data). Model terms are: 'cl' = carapace length, 'days' = days since the start of the experiment, 'lob_id' = a unique identifier for each lobster. The optimal model is in bold.

ID	Model structure	LOO IC	SE LOO IC	Predicted annual growth in mm CL yr^{-1} (95% credible interval)
mah5	**CL ~ s(days, k = 3) + (days | lob_id)**	**1323.6**	**24.9**	–
mah4	CL ~ days + (days | lob_id)	1387.6	26.4	20.9 (19.8–22.0)
mah3	CL ~ days + (1 | lob_id)	1489.3	34.4	20.9 (19.8–22.0)
mah2	CL ~ days	1886.4	30.9	20.8 (20.2–21.5)
mah1	CL ~ 1	2489.7	21.7	–

7. DISCUSSION

7.1 Limitations of this analysis

There are two primary limitations to this analysis:

1. there is limited spatial coverage of juvenile growth information, with the best information coming from Stewart Island (i.e., the southernmost fished area around New Zealand); and
2. the temporal coverage is also limited, except at Stewart Island where the data extend over a 19-year period (however, there are no recent data).

Regarding the first limitation, by far the best existing growth information for juvenile red rock lobsters around New Zealand comes from the diver survey of size composition in Halfmoon Bay, Stewart Island (within CRA 8). Based on these data, the time lag between settlement and recruitment to stock assessment models would be around 2.5 years, when this occurs at 30–35 mm TW. However, this was based on growth information at the cold-water end of their distribution around New Zealand, and increased growth rate should be expected further north with increased temperature (Hooker et al. 1997), shortening the time lag to recruitment. This is supported by the faster growth rate estimated at Gisborne Wharf (CRA 3) from length-based information and relatively fast growth at CRA 1 and CRA 2 based on fishery tag information. Hence, the lag time may be closer to 2 years in these warmer QMAs.

Regarding the second limitation, the authors did not model interannual variation in juvenile growth rate or explore the processes that might cause this, such as density dependent effects or changes in environmental conditions. Some regions of New Zealand have experienced a large degree of warming since the late-1970s, particularly off the east coasts of both the North Island and South Island (Sutton & Bowen 2019), which may have affected juvenile growth rates and the time lag to recruitment.

7.2 Comparison of growth estimates

Estimates of juvenile growth rate were obtained from the analysis of size composition data from Halfmoon Bay, which were corroborated by independent mark-recapture information from the same location. This increases confidence that the length-based growth estimates were unbiased, noting that potential temporal variation in growth rate was not accounted for. The annual CL increment at 30 mm TW for length-based Halfmoon Bay growth model (*lf_hm_7*) was 16.7 mm for males (95% CI = 9.5–24.4 mm CL) and 15.3 mm for females (95% CI = 7.7–22.9 mm CL); and for Gisborne (*lf_gw_4*) was 19.1 mm CL across both sexes (95% CI = 14.3–23.7 mm CL). These growth rates are broadly consistent with estimates from other studies of this species, noting that spatial and temporal variability in growth rate is likely, e.g.,

- Annala & Bycroft (1985), who estimated ~35 mm of CL growth across two years (~17.5 mm CL per year), using an earlier subset of the Halfmoon Bay data; and
- Linnane et al. (2012), who estimated an annual growth increment of 16.8-19.7 mm CL for males across the species range in Australia and 10.0–14.1 mm CL growth for females, at a starting size of 60 mm CL (i.e., slightly above 30 mm TW around New Zealand).

The fishery tag-recapture based growth information indicate that growth rates may be much faster in CRA 1 and CRA 2, than QMAs to the south. Thus, differences in growth rates between studies may, in part, reflect differing environmental conditions between study sites, particularly in comparisons of studies in warm versus colder parts of the species range.

7.3 Implications for stock assessment

The Fisheries New Zealand Rock Lobster Working Group (RLWG) agreed that the tank-based growth study of captive lobsters, which were given replete food resources, could be used to inform the upper bound of growth around the size-at-recruitment to stock assessment models, with the intention of constraining growth to realistic values. The mean growth of wild lobsters at Gisborne Wharf (~12 mm TW or ~19 mm CL growth annually at 30 mm TW) was slightly below the mean annual growth rate from the tank-based study (~21 mm CL annually) (noting that the non-linear model from the tank-based study indicated that the lobsters can actually grow faster than this). However, sea surface temperatures have increased in this region since the late-1970s (Sutton & Bowen 2019) when the Gisborne Wharf growth study was undertaken (McKoy & Esterman 1981). Furthermore, the fishery tag-based growth information suggests even faster growth in CRA 1 and CRA 2 (Figure A.8), the QMAs with the warmest sea temperatures, than in CRA 3 and the colder QMAs to the south. Therefore, it is recommended that the growth increment posteriors for Halfmoon Bay (Figure 5) are only used to develop growth priors for cooler QMAs (i.e., CRA 6–8), and that the Gisborne growth increment posteriors (Figure 8) should only be used for warmer QMAs, except for CRA 1–2 where the fishery tag data still contain the best information of juvenile growth. Given the lack of contrast in the TW-based growth of males and females (the increased growth rate of males in terms of CL is largely negated by the larger different CL-TW relationships of males and females), the same prior could be used for each sex.

Using juvenile growth information to estimate the time lag from puerulus settlement to recruitment in the stock assessment model appears to be a better approach than using puerulus randomisation trials to guide this lag, which has, in the past, sometimes resulted in biologically unrealistic time lags. However, the randomisation trials still have some utility for assessing whether the puerulus indices contain a coherent signal (with the fishery-based information) of recruitment variation through time, when biologically realistic time lags are used.

7.4 Puerulus settlement indices

It was hoped that an improved representation of the time lag from puerulus settlement to recruitment in the stock assessment model would produce improved model fits to puerulus data. However, specifying a three-year lag did not substantively improve model fits to the puerulus indices for either of the latest assessments for CRA 4 and CRA 5 (Rudd et al. 2021b, Webber et al. 2021). Having eliminated the possibility that poor fits to the puerulus indices might be driven by mis-specification of juvenile growth, it now seems more likely that the puerulus indices in their present form are not representative of recruitment to some if not all of the stocks as represented by the stock assessment models. Some possible explanations for this include:

- Locating puerulus collectors in places that are not representative of recruitment to the stock (i.e., the locations for deployment are often calm locations so that collectors are not destroyed in inclement weather).
- Not representing processes that could affect relative recruitment strength between settlement and recruitment to the fishery (e.g., disease, major seismic events, or changes in environmental conditions and food availability).
- Recruitment to these stocks, as estimated by the stock assessment model, is poorly estimated.

Relating to the first point, previous analyses found evidence for positive correlation in annual settlement patterns when comparing collector sites in adjacent QMAs (e.g., Andy MacKenzie, NIWA, unpublished data). Thus, temporal recruitment patterns may be shared across coastal regions. However, it is entirely plausible that recruitment patterns at the puerulus collectors could differ from the fished region of the stock within same QMA, e.g., where these are separated by strong hydrographic or geographic features.

Relating to the second point, density-dependent mortality should increase the mortality rate of relatively strong cohorts (Moyle et al. 2009). The shape of this density-dependent mortality response could potentially be estimated by assessment models, informed by model fit to the puerulus indices, or could be determined from a review of studies assessing the effects of density on mortality rate. This would have the effect of dampening peaks in recruitment from the puerulus series and this could be configured to affect only mortality rate in the first-year post-settlement, based on the findings of Breen & Booth (1989).

7.5 Future research recommendations

7.5.1 Stock assessment

Based on this juvenile growth analysis, the following recommendations are made for future stock assessments of New Zealand red rock lobster stocks:

- the priors for the annual growth increment at small sizes (e.g., *Galpha*) should be based on growth increment posteriors from this study (Table 5). For example, the Halfmoon Bay posteriors for growth at 30 mm TW could be used for colder-water QMAs (e.g., CRA 6–8), and the Gisborne Wharf posterior could be used for warmer QMAs (e.g., CRA 3) (Figure 5). Priors may need to be modified for CRA 1 and CRA 2, where lobsters appear to grow faster than in the other QMAs;
- specifying a 2 or 3 year time lag from settlement to recruitment in stock assessment models, if the mean size is within the range of 30–35 mm TW, favouring 2 years for warmer QMAs, including CRA 1–4; and
- specifying a standard deviation of at least 2.5 mm TW for size-at-recruitment if the mean size is within the range of 30–35 mm TW.

Table 5: Summary of tail-width increment posteriors that could be used for developing growth model priors for red rock lobsters (e.g., *Galpha*) by QMA. For CRA 1–2, the corresponding annual growth increments at 30–40 mm tail width are likely to be greater than for CRA 3–4. Annual growth increments in CRA 5 may be between those stated for QMAs to the north and south, based on sea surface temperature. Note that sex-specific growth increment priors do not appear to be required at these sizes.

			Starting	Annual tail-width increment (mm)				
QMA	Model	Sex	size (mm tail width)	Mean	SD	2.5%	Median	97.5%
CRA 3–4	*lf_gw_4*	Both	30	11.66	1.54	8.71	11.66	14.65
			40	11.77	1.55	8.71	11.80	14.79
CRA 6–8	*lf_hm_7*	Male	30	8.86	1.95	0.90	8.86	12.68
			40	7.79	2.13	3.55	7.83	12.01
		Female	30	8.68	2.11	4.39	8.69	12.69
			40	7.51	2.44	2.52	7.53	12.30

7.5.2 Growth estimation

Diver surveys of size distribution appear to be an effective means of informing juvenile growth to a high level of precision, although they are expensive and may take many years of sampling to generate precise growth estimates. Hence, future efforts to inform the estimation of juvenile growth (e.g., at locations other than Halfmoon Bay and Gisborne) may need to consider alternative means for informing the estimation of juvenile growth, including:

- tank-based growth experiments, noting that it may be difficult to accurately simulate the environmental/food conditions experienced by wild lobsters; and
- direct ageing (e.g., Gnanalingam et al. 2018), which can integrate growth information from pre- and post-recruited lobsters and would ideally include some validation with known-age lobsters.

8. ACKNOWLEDGEMENTS

This research was funded by Fisheries New Zealand, who awarded the contract for part of this work to the New Zealand Rock Lobster Industry Council Ltd under CRA2019-01; and part of this work was awarded to Quantifish Ltd under CRA2020-01.

We thank Paul Breen (Breen Consulting), John Booth, Jeff Forman (NIWA), and Graeme Moss (NIWA) for providing unpublished lobster measurements. We also acknowledge the work of John McKoy, John Annala, and Bruce Bycroft who conducted earlier growth analyses of juvenile red rock lobsters around New Zealand, including the collection of mark-recapture data used by this analysis. We thank Mark Edwards and Daryl Sykes for encouragement, Helen Regan for logistic support, and members of the Rock Lobster Working Group for their advice. And we thank the other members of the New Zealand rock lobster stock assessment team, including Maite Pons, Merrill Rudd, and Paul Starr, for their support and input throughout.

9. REFERENCES

Annala, J.H.; Bycroft, B.L. (1985). Growth rate of juvenile rock lobsters (*Jasus edwardsii*) at Stewart Island, New Zealand. *New Zealand Journal of Marine and Freshwater Research 19*: 445–455.

Booth, J.D. (1979). Settlement of the rock lobster, *Jasus edwardsii* (Decapoda: Palinuridae), at Castlepoint, New Zealand. *New Zealand Journal of Marine and Freshwater Research 13*: 395–406.

Booth, J.D.; Forman, J.S.; Stotter, D.R. (1998). Abundance of early life history stages of the red rock lobster, *Jasus edwardsii*, with management implications. *New Zealand Fisheries Assessment Research Document 98/10*. 71 p.

Breen, P.A.; Booth, J.D. (1989) Puerulus and juvenile abundance in the rock lobster *Jasus edwardsii* at Stewart Island, New Zealand (Note). *New Zealand Journal of Marine and Freshwater Research 23*: 519–523.

Bürkner, P. (2017). brms: An R Package for Bayesian Multilevel Models Using Stan. *Journal of Statistical Software 80*: 1–28.

Forman, J.; McKenzie, A.; Stotter, D. (2020). Settlement indices for 2017/18 fishing year for the red rock lobster (*Jasus edwardsii*). *New Zealand Fisheries Assessment Report 2019/54*. 41 p.

Gnanalingam, G.; Butler, M.J., IV; Matthews, T.R.; Hutchinson, E.; Kilada, R. (2018). Directly ageing the Caribbean spiny lobster, *Panulirus argus*, with validated band counts from gastric mill ossicles. *ICES Journal of Marine Science 76*: 442–451.

Haist, V.; Breen, P.A.; Edwards, C.T.T. (2015). The 2014 stock assessment of rock lobsters (*Jasus edwardsii*) in CRA 3, and development of new management procedures. *New Zealand Fisheries Assessment Report 2015/28*. 73 p.

Hooker, S.H.; Jeffs, A.G.; Creese, R.G.; Sivaguru, K. (1997). Growth of captive *Jasus edwardsii* (Hutton) (Crustacea: Palinuridae) in north-eastern New Zealand. *Marine and Freshwater Research 48*: 903–909.

Linnane, A.; Hobday, D.; Frusher, S.; Gardner, C. (2012). Growth rates of juvenile southern rock lobster (*Jasus edwardsii*) estimated through a diver-based tag–recapture program. *Marine and Freshwater Research 63*: 110–118.

Mackay, K.A.; George, K. (2002). Database documentation: rlcs. (A) Catch sampling schema. NIWA Internal Report. 53 p.

McKoy, J.L.; Esterman, D.B. (1981). Growth of rock lobsters (*Jasus edwardsii*) in the Gisborne region, New Zealand. *New Zealand Journal of Marine and Freshwater Research 15*: 121–136.

Moyle, K.; Johnston, D.; Knott, B.; Melville-Smith, R.; Walker, D. (2009). Effect of stocking density on the growth, survival, and behavior of postpuerulus Western rock lobster, *Panulirus cygnus* (George) (Decapoda: Palinuridae). *Journal of the World Aquaculture Society 40*: 255–265.

R Core Team (2019). *R: A language and environment for statistical computing*. R Foundation for Statistical Computing: Vienna, Austria. Available at: https://www.R-project.org/

Rudd, M.B.; Pons, M.; Roberts, J.; Webber, D.N.; and Starr, P.J. (2021b). The 2020 stock assessment of red rock lobsters (*Jasus edwardsii*) in CRA 4. *New Zealand Fisheries Assessment Report 2021/80.* 112 p.

Rudd, M.B.; Roberts, J.; Large, K.; Webber, D.N.; Starr, P.J. (2021a). The 2019 stock assessment of rock lobsters (*Jasus edwardsii*) in CRA 1. *New Zealand Fisheries Assessment Report 2021/04*. 101 p.

Sutton, P.J.H.; Bowen, M. (2019). Ocean temperature change around New Zealand over the last 36 years. *New Zealand Journal of Marine and Freshwater Research 53*: 305–326.

Vehtari, A.; Gelman, A.; Gabry, J. (2017). Practical Bayesian model evaluation using leave-one-out cross-validation and WAIC. *Statistics and Computing 27*: 1413–1432.

Webber, D.N.; Roberts, J.; Pons, M.; Starr, P.J.; Rudd, M.B. (2021). The 2020 stock assessment of red rock lobsters (*Jasus edwardsii*) in CRA 5. *New Zealand Fisheries Assessment Report 2021/62*. 91 p.

Webber, D.N.; Roberts, J.; Rudd, M.B.; Starr, P.J.; Large, K. (2020). The 2019 stock assessment of rock lobsters (*Jasus edwardsii*) in CRA 3. *New Zealand Fisheries Assessment Report 2020/42*. 93 p.

Wickham, H. (2017). *tidyverse: Easily Install and Load the "Tidyverse"*. R package version 1.2.1. Available at: https://CRAN.R-project.org/package=tidyverse

Wood, S.N. (2011). Fast stable restricted maximum likelihood and marginal likelihood estimation of semi-parametric generalized linear models. *Journal of the Royal Statistical Society B 73(1)*: 3–36.

APPENDIX A. OBSERVATIONS

Carapace length and tail width

Paired carapace and tail width measurements of juvenile lobsters from diver surveys at Halfmoon Bay in 1986 and 1987 were provided by Paul Breen, aggregated across all survey sites. These comprised 157 males and 150 females, ranging from 20 to 102 mm CL (Figure A.1).

A small sample of paired carapace length-tail width measurements were collected using diver surveys at Gisborne in December 1999 and January 2000, which were provided by John Booth in the form of a scanned scatterplot. This plot was digitised for the current analysis. Apart from a small number of larger lobsters (i.e., > ~70 mm TW), these were all unsexed. The total sample size of paired measurements was 71 individuals, including 6 females, 2 males, and 63 unsexed lobsters (Figure A.1).

A much larger sample of post-recruit carapace length-tail width measurements were recorded by the fishery and were extracted from the *rlcs* database (Table A.1 and Figure A.2). Nearly all of the paired CL-TW measurements were from fishing seasons 1986–87 to 1997–98, with a small number in 2016–17. These data were not used to convert carapace length to tail width, although inferences were made about spatial patterns in this relationship at the QMA-level.

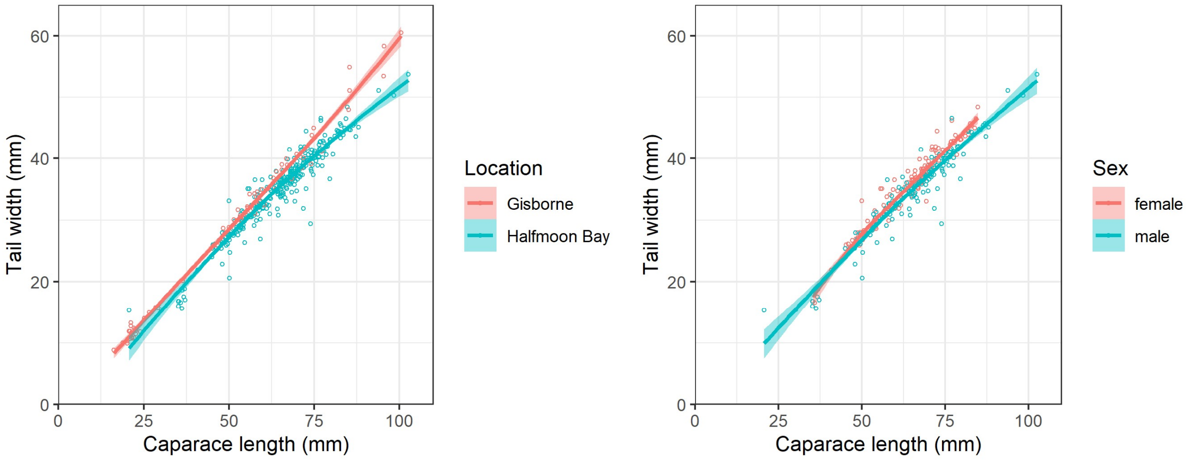

Figure A.1: Carapace length (CL) to tail width (TW) relationship of juveniles from diver surveys by location of sampling (left) and by sex at Halfmoon Bay, Stewart Island (right). Open circles are raw observations; lines with shaded areas are LOESS smoothers fitted to these data and 95% confidence intervals of these smooths.

Table A.1: Number of commercial pot fishery paired measurements of carapace length (CL) and tail width (TW) summarised by CL bin, QMA of capture and sex (*rlcs* database). This table only includes lobsters of between 30–100 mm CL.

	QMA								Sex	
Carapace length bin (mm)	CRA 2	CRA 3	CRA 4	CRA 5	CRA 6	CRA 7	CRA 8	CRA 9	Female	Male
(30, 40]	0	0	2	0	1	0	0	0	2	1
(40, 50]	0	2	6	0	1	0	3	0	8	4
(50, 60]	0	15	92	23	1	27	6	0	88	76
(60, 70]	1	270	1 125	463	13	802	568	0	2 211	1 059
(70, 80]	76	4 174	6 768	2 604	35	4 211	5 398	2	15 874	7 585
(80, 90]	644	20 192	25 287	7 921	556	4 726	34 143	52	65 863	28 495
(90, 100]	1208	35 074	36 303	9 486	1 977	3 018	69 599	60	65 908	92 951

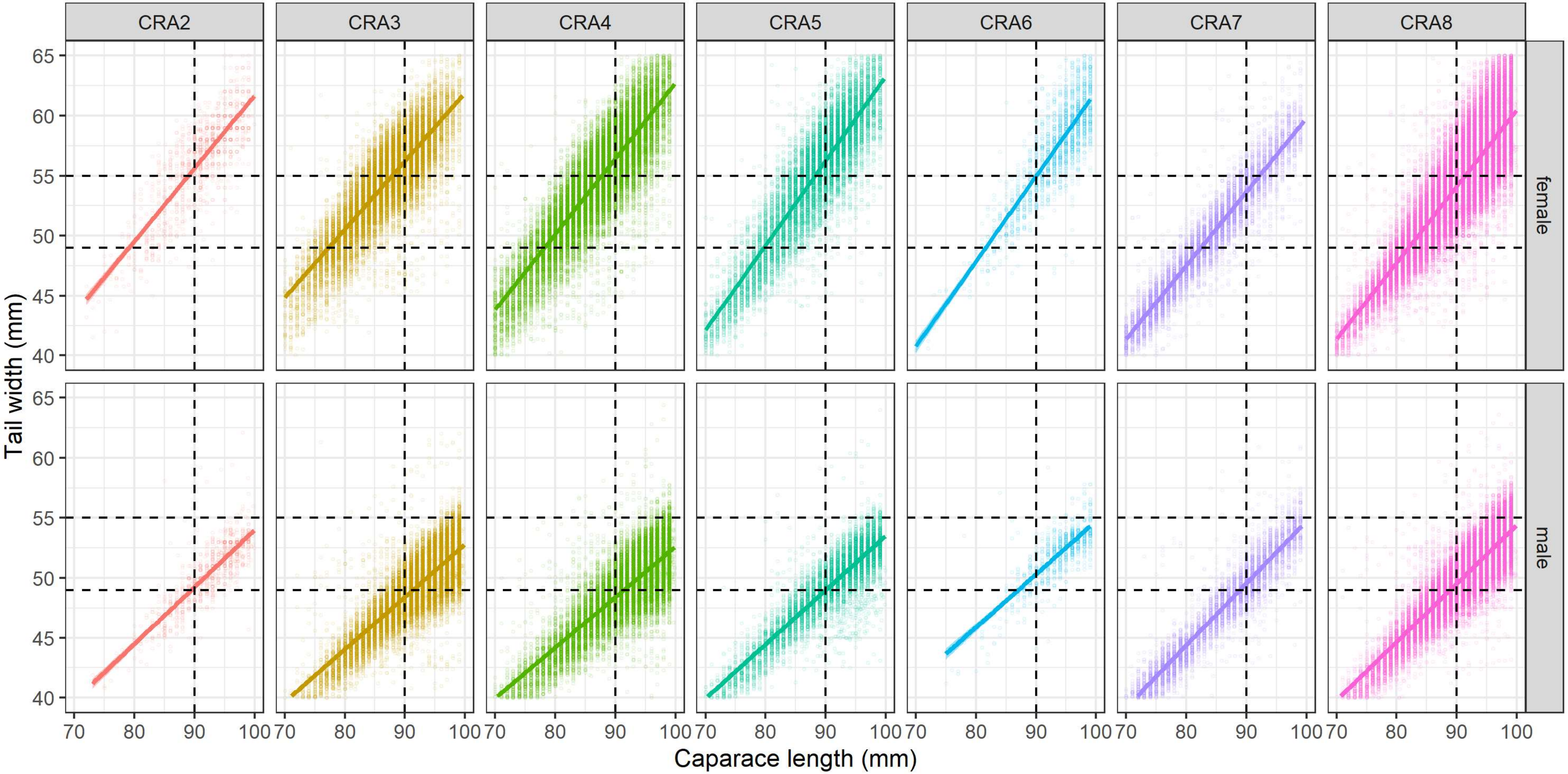

Figure A.2: Carapace length to tail width relationship of post-recruits recorded in the *rlcs* database, by sex and QMA of capture, excluding lobsters larger than 100 mm carapace length and a small number of lobsters recorded in CRA 1 and CRA 9. Points represent individual paired measurements, to which a linear model was fitted by QMA (lines) with 95% confidence interval (shaded area). The dashed reference lines are placed to highlight variability in the carapace length-tail width relationship by sex and QMA.

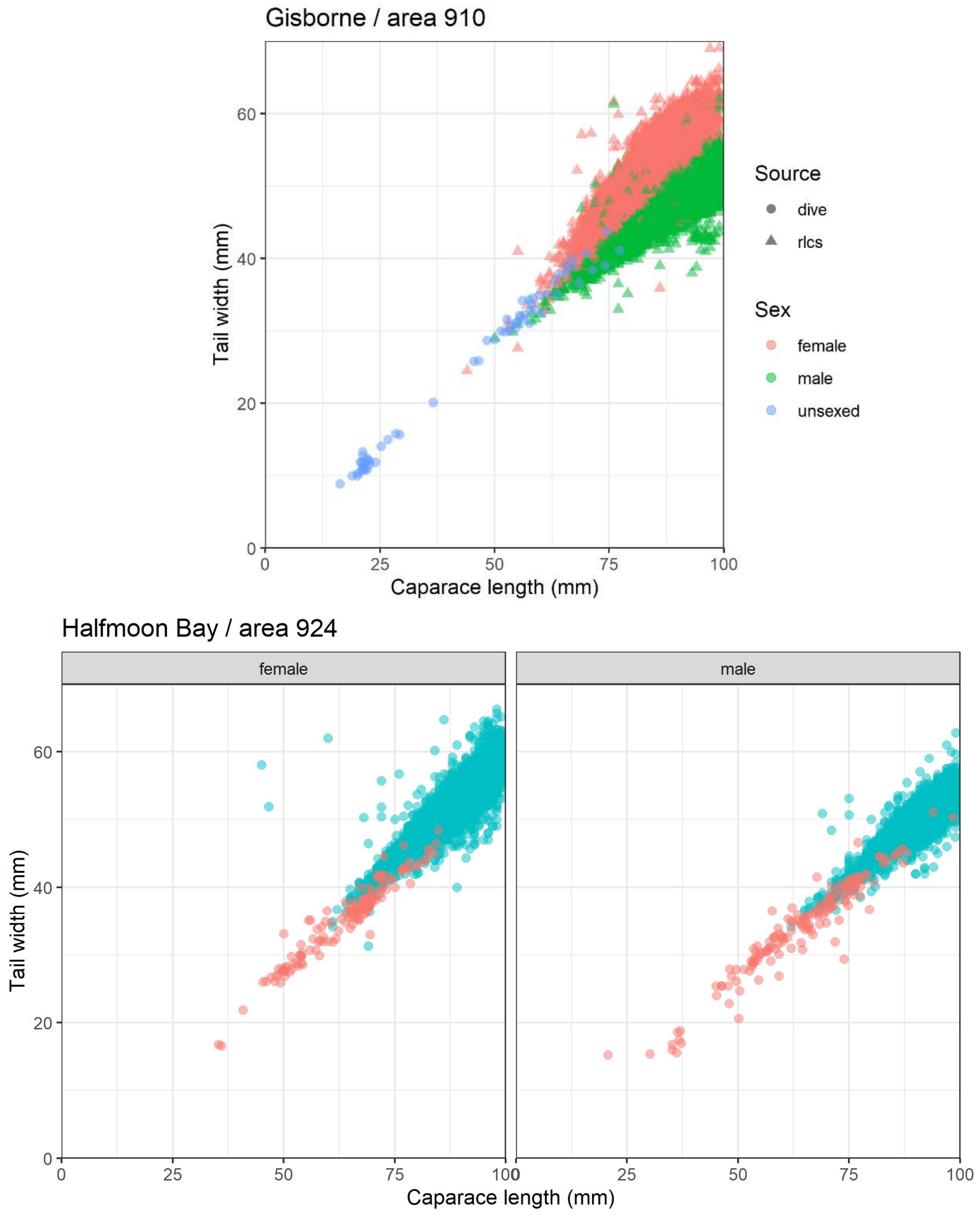

Figure A.3: Carapace length to tail width relationship from diver surveys ('dive') and fishery catch sampling ('rlcs') for Gisborne (top) and Halfmoon Bay, Stewart Island (bottom).

Size distribution data

Halfmoon Bay, Stewart Island

The size distribution of juvenile lobsters was monitored by diver surveys at Halfmoon Bay, Stewart Island. Surveys were done in all years from 1982 to 2000, with monitoring in winter months in all years. During these surveys, divers collected juveniles in shallow water at a set of fixed sites in and around Halfmoon Bay. At the surface, the carapace length (CL) of the collected lobsters was then measured to the nearest 0.1 mm (although, to 1 mm in at least one survey) using vernier callipers. The data were extracted from electronic files held by Paul Breen (1982–1996) and Jeff Forman (1997), who provided sex-disaggregated length frequencies from surveys in winter months (June in most years, but also May, August, and July in some years). For these years, the individual CL measurements were rounded down to the nearest 1 mm, and the data were summed for 1 mm CL bins, for each survey year and sex. The data for 1998–2000 were extracted from the *rocklob* database, in which counts were summarised in 5 mm CL bins (Table A.2).

Table A.2: Summary of lobsters sampled for carapace length by a diver survey at Halfmoon Bay, Stewart Island, in winter months of 1982–2000.

		Sum of lobsters measured			
Year	Sampling months	Females	Males	Resolution (mm)	Source
1982	June	146	152	1	P. Breen
1983	May, June	372	392	1	P. Breen
1984	June	392	442	1	P. Breen
1985	June	528	524	1	P. Breen
1986	June	477	510	1	P. Breen
1987	June	178	171	1	P. Breen
1988	June	77	70	1	P. Breen
1989	May, June	217	219	1	P. Breen
1990	June	235	232	1	P. Breen
1991	June	285	352	1	P. Breen
1992	August	264	294	1	P. Breen
1993	June	405	471	1	P. Breen
1994	June	430	495	1	P. Breen
1995	June	237	280	1	P. Breen
1996	June	340	391	1	P. Breen
1997	July	309	401	1	J. Forman
1998	July	460	512	5	*rocklob* database
1999	July	441	456	5	*rocklob* database
2000	July	323	389	5	*rocklob* database

Figure A.4: Size composition data of female juvenile red rock lobsters sampled by diver surveys at Halfmoon Bay, Stewart Island in the winters of 1982–2000. Measurements for 1982–1997 were available to a 1 mm resolution (Paul Breen unpublished data, Jeff Forman unpublished data) and to a 5 mm resolution for 1998–2000 (*rocklob* database).

Figure A.5: Size composition data of <u>male</u> juvenile red rock lobsters sampled by diver surveys at Halfmoon Bay, Stewart Island in the winters of 1982–2000. Measurements for 1982–1997 were available to a 1 mm resolution (Paul Breen unpublished data, Jeff Forman unpublished data) and to a 5 mm resolution for 1998–2000 (*rocklob* database).

Gisborne

The size distribution of juvenile lobsters at Gisborne Wharf was sampled at irregular time intervals from 1976–1979 (a total of eight surveys) (see McKoy & Esterman 1981 for a summary of methods and data). This study produced unsexed length-frequency distributions, which were plotted to a 5 mm resolution, ranging from 20 to 100 mm CL (see figure 2 of McKoy & Esterman 1981). These data were digitised for the purposes of re-analysis by the current study (Table A.3 and Figure A.6).

Table A.3: Summary of lobsters sampled for carapace length by a diver survey at Gisborne Wharf, Gisborne, 1976–1979. All measurements were digitised from figure 2 of McKoy & Esterman (1981).

Sampling month-year	Sum of lobsters measured (all unsexed)
Feb-1976	211
Oct-1976	187
Mar-1977	176
Oct-1977	164
Jul-1978	93
May-1979	104
Aug-1979	146
Oct-1979	51

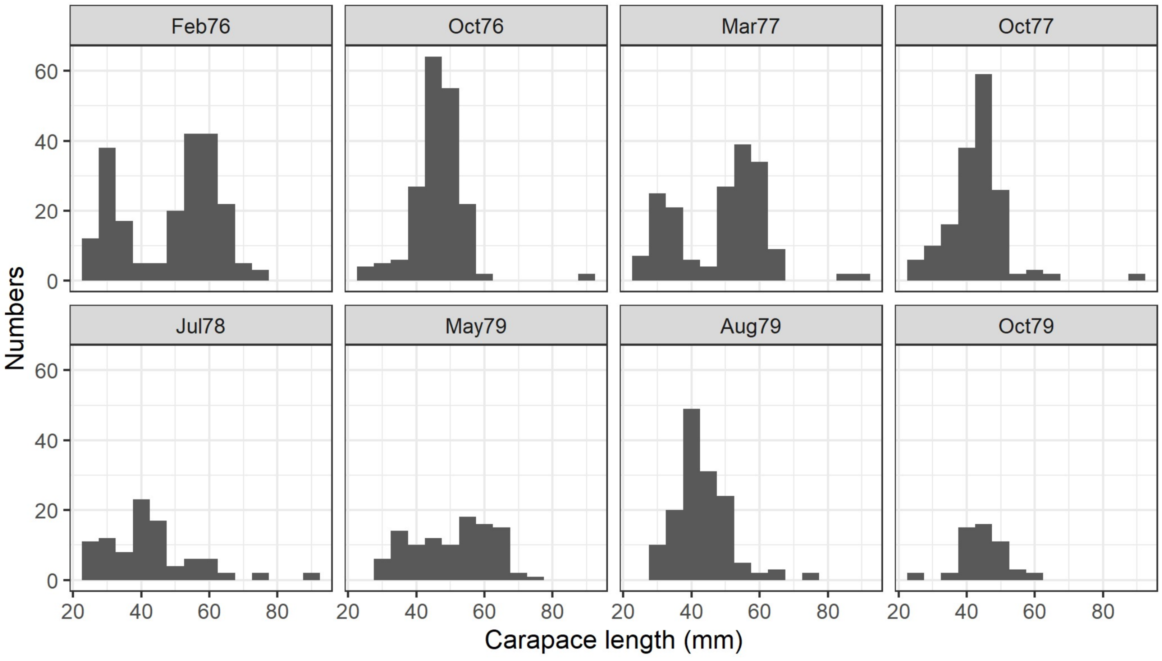

Figure A.6: Unsexed size composition data of juvenile red rock lobsters sampled by diver surveys at Gisborne Wharf 1976–1979 (digitised from a plot of McKoy & Esterman 1981).

Wellington Harbour

The size distribution of juvenile lobsters at a number of sites around Wellington Harbour was sampled in multiple months each year from April 1993–August 2001 (see Booth et al. 1998 for a summary of methods and data). These data were extracted from the *rocklob* database, where they were unsexed and summarised to a 5 mm resolution, ranging from 30 to 90 mm CL.

Based on a preliminary exploration of the data from all Wellington harbour sampling sites, it was determined that only data collected from the Kaiwharawhara monitoring site (*rocklob* location code WTN01J) in 1993–1995 might contain usable size-based growth information. The data collected from this site are summarised in Table A.4 and Figure A.7. Data were also collected in subsequent years (up to 2001) at Wellington Harbour sites (including WTN01J); there were very few samples of lobsters smaller than 70 mm carapace length due to poor recruitment and these were excluded from the current analysis.

For all other monitoring sites around Wellington Harbour (Moa Point, Palmer Head, Island Bay, and Worser Bay) it was determined from visual inspection of length-frequency distributions that there was no coherent growth information at any of these sites across sampling periods.

Table A.4: Summary of lobsters sampled for carapace length by a diver survey at Kaiwharawhara, Wellington Harbour, 1993–1995. All measurements were extracted from the *rocklob* database, where they were available at a 5 mm carapace length resolution.

Sampling month-year	Sum of lobsters measured (all unsexed)
Jul-1993	106
Jan-1994	83
Jun-1994	483
Dec-1994	201
Jun-1995	263
Dec-1995	97

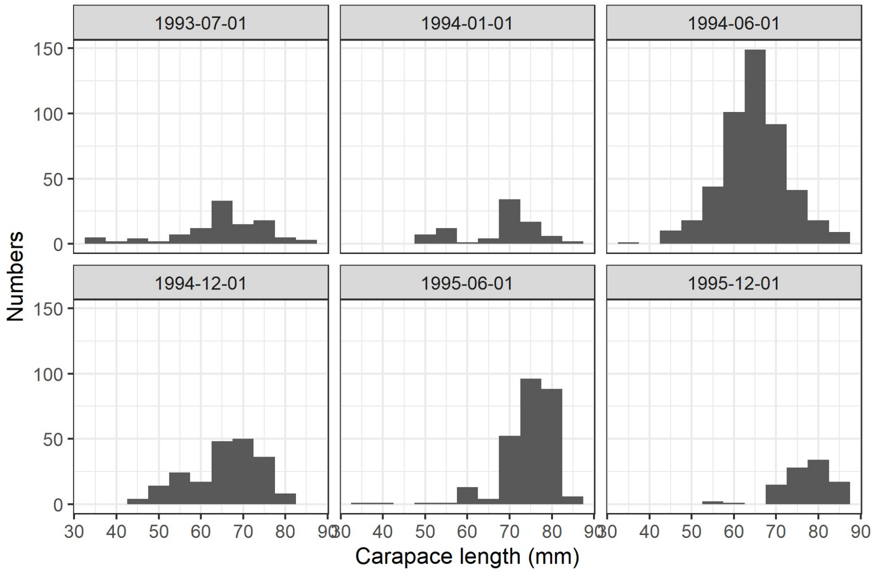

Figure A.7: Unsexed size composition data of juvenile red rock lobsters sampled by diver surveys at Kaiwharawhara, Wellington Harbour in summer and winter months of 1993–1995 (data from *rocklob* database; sampling methods and relevant data summaries by Booth et al. 1998).

Mark-recapture data

Diver survey mark-recapture data

Mark-recapture size increment data were digitised from figure 4 of Annala and Bycroft (1985), which gives a description of sampling methods and data preparation. Briefly, these data include the growth increments of rock lobsters recaptured by a diver survey at Halfmoon Bay, Stewart Island, which marked lobsters between the winters of 1982 and 1984, and where "the month of release was identified by the pleopod clipped, and the year of release was inferred from the increase in CL and the regeneration of the clipped pleopod". These data comprised 386 growth increment records of lobsters ranging from 25 to 70 mm CL at the time of release, spending either 3, 6, 9, 12, 15, or 18 months at liberty (Annala & Bycroft 1985). Both the size-at-release and growth increment data were recorded to a 5 mm resolution (Table A.4 and Table A.5).

Table A.5: Size-at-release of lobsters recaptured by a mark-based growth study of juvenile red rock lobsters at Halfmoon Bay, Stewart Island, in 1982–1984 (Annala and Bycroft 1985).

Months spent at liberty	Numbers in each at size-at-release bin (midpoint of each bin in mm carapace length)																		
	Females									Males									Total
	25	30	35	40	45	50	55	60	65	25	30	35	40	45	50	55	60	65	
3	0	1	0	6	21	10	21	13	6	0	3	2	11	19	16	13	22	9	173
6	0	0	4	2	6	3	7	4	2	0	0	2	3	6	12	10	9	6	76
9	0	1	0	6	7	7	4	2	2	0	2	0	2	4	5	4	2	0	48
12	0	0	0	4	11	4	4	0	1	2	0	1	4	14	10	3	3	3	64
15	0	1	0	3	2	1	2	1	0	0	0	0	4	3	3	0	1	0	21
18	0	0	0	0	1	1	0	0	0	0	0	0	0	0	1	1	0	0	4

Table A.6: Growth increment of lobsters recaptured by a mark-based growth study of juvenile red rock lobsters at Halfmoon Bay, Stewart Island, in 1982–1984 (Annala & Bycroft 1985).

Months spent at liberty	Numbers in each growth increment bin (midpoint of each bin in mm carapace length)														
	Females							Males							Total
	0	5	10	15	20	25	30	0	5	10	15	20	25	30	
3	45	29	4	0	0	0	0	52	35	6	2	0	0	0	173
6	7	16	4	1	0	0	0	6	28	12	2	0	0	0	76
9	1	9	9	4	5	1	0	0	3	9	6	0	1	0	48
12	0	0	5	10	7	2	0	0	3	7	14	13	2	1	64
15	0	1	1	4	3	0	1	0	0	0	4	4	3	0	21
18	0	0	0	1	1	0	0	0	0	1	0	0	1	0	4

Fishery tag-recapture data

Fishery tag-recapture size increment data were extracted from the *tag* database, including all recaptures up to the 2018–19 fishing season. These data were primarily informative of growth between 40 and 70 mm tail width (Table A.7). For each linked recapture event, annualised growth increment was derived as the total growth increment divided by years spent at liberty. The annual increment was then plotted by release tail width, QMA, and sex (Figure A.8), using a subset of tags spending at least one year at liberty, to minimise potential biases associated with the timing of tag release-recapture relative to the main moulting periods (e.g., as by Webber et al. 2020).

Table A.7: Number of commercial pot fishery tag recaptures by tail width (mm TW) bin and QMA of release and sex (*tag* database).

	QMA									Sex	
TW release	CRA 1	CRA 2	CRA 3	CRA 4	CRA 5	CRA 6	CRA 7	CRA 8	CRA 9	Female	Male
(15, 20]	0	0	0	0	0	0	0	0	0	0	0
(20, 25]	0	0	0	0	0	0	0	1	0	1	0
(25, 30]	0	0	1	0	0	0	0	0	0	1	0
(30, 35]	0	0	15	0	1	0	0	1	0	12	5
(35, 40]	5	2	141	3	7	0	69	18	0	71	174
(40, 45]	31	6	523	13	88	0	264	119	0	352	692
(45, 50]	185	234	1 604	126	764	1	270	999	1	829	3 355
(50, 55]	545	1 099	2 406	1 737	2 923	22	161	4 030	19	2 420	10 522
(55, 60]	540	1 370	601	756	1 740	23	43	2 848	13	3 920	4 014
(60, 65]	349	935	254	332	901	26	21	1 344	8	2 530	1 640
(65, 70]	251	493	63	104	458	19	5	755	24	1 520	652
(70, 75]	155	260	17	33	271	24	3	372	22	882	275
(75, 80]	71	93	7	12	120	14	1	152	15	381	104
(80, 85]	26	23	0	2	51	18	1	76	15	184	28
(85, 90]	5	6	1	2	17	23	0	20	8	75	7
(90, 95]	0	0	0	0	6	8	0	14	1	28	1
(95, 100]	0	1	0	1	6	3	0	3	0	13	1
(100, 105]	0	0	0	0	1	0	0	5	0	5	1
(105, 110]	0	0	0	0	0	0	0	0	0	0	0

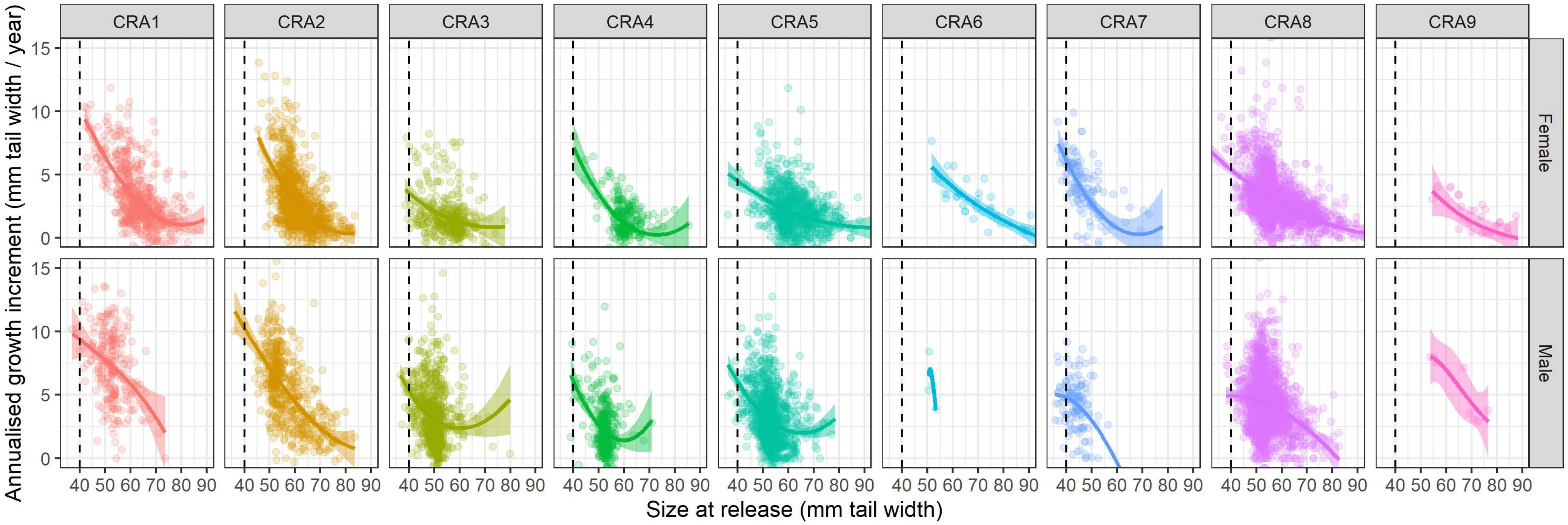

Figure A.8: LOESS smoothers (lines) fitted to the annualised size increment of red rock lobsters tagged by the fishery, by size, and QMA at release, using a subset of lobsters spending at least 1 year at liberty (points) (data from *rlcs* database). Shaded areas are 95% confidence intervals of the smoothers.

Mahanga Bay (NIWA) tank-based growth study

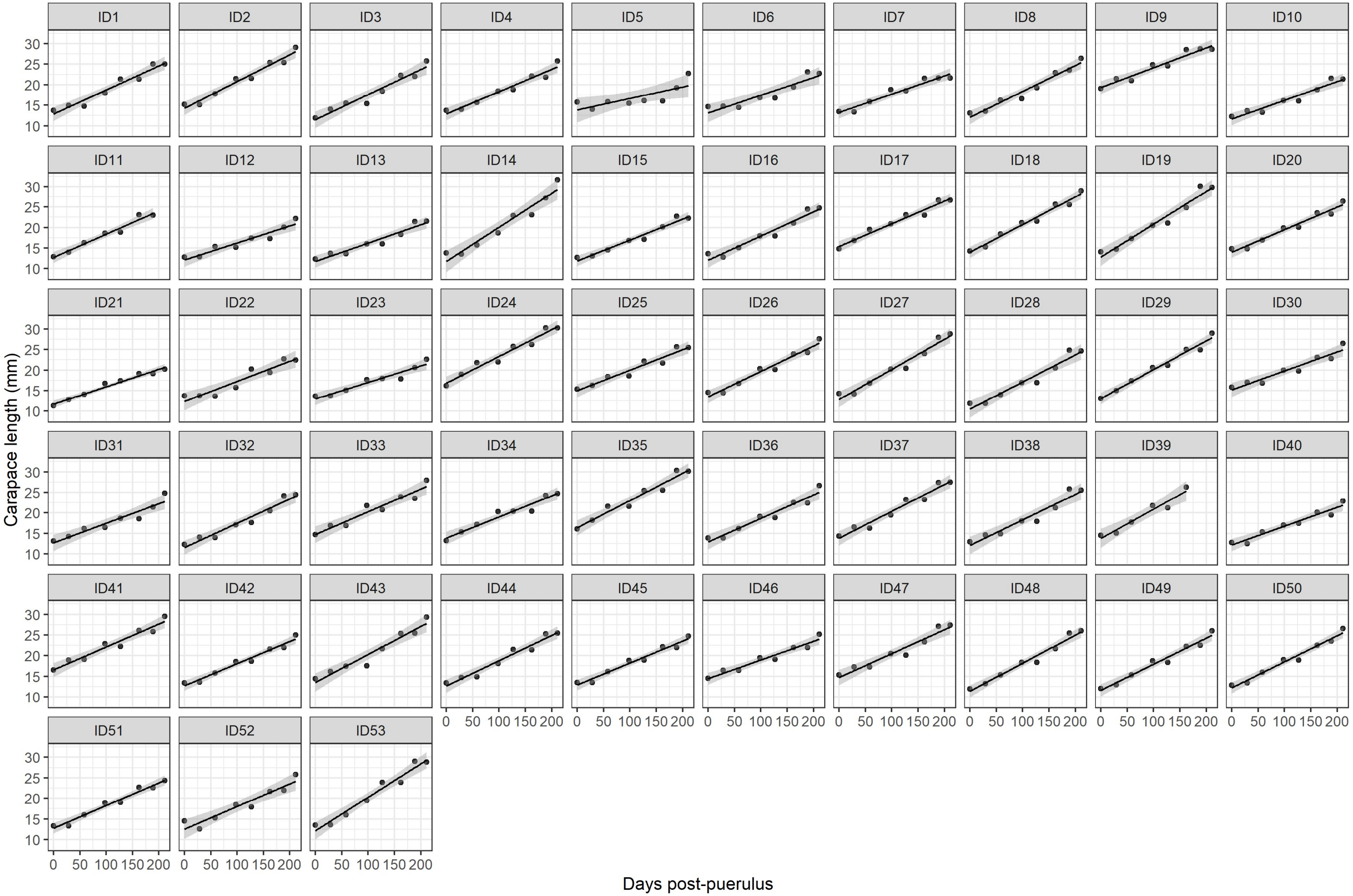

Figure A.9: Growth of individual post-pueruli red rock lobsters (labelled with lobster ID) in a longitudinal tank-based growth study of captive lobsters at NIWA, Mahanga Bay, Wellington (Graeme Moss, NIWA, unpublished data). Points are individual measurements, lines are linear models fitted to these points, and shaded areas are 95% confidence intervals.

APPENDIX B. MODEL DIAGNOSTIC PLOTS

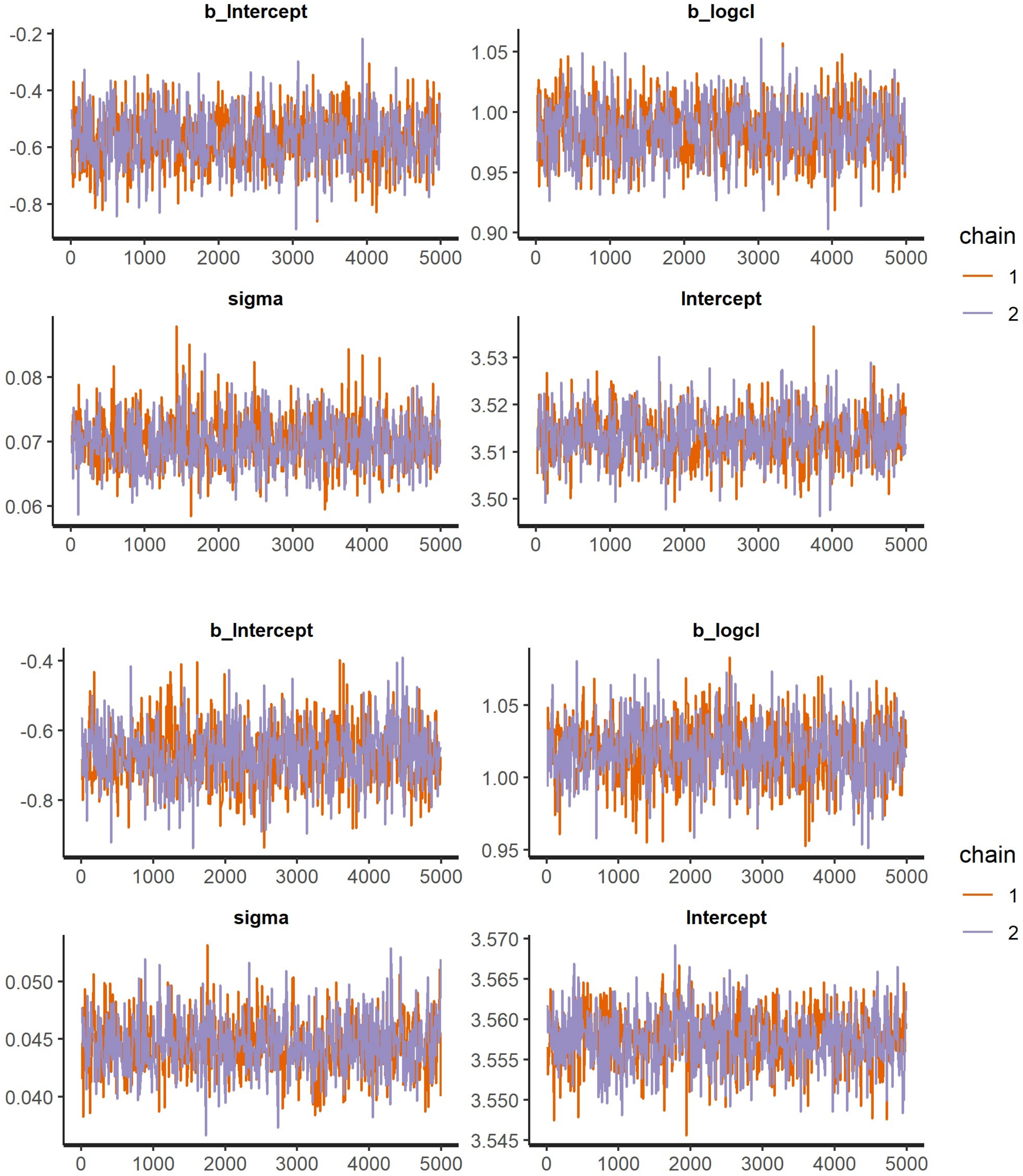

Figure B.1: MCMC trace plots for linear models estimating the tail width of red rock lobster at Halfmoon Bay, Stewart Island given carapace length for females (top; model *tw_f*) and males (bottom; model *tw_m*).

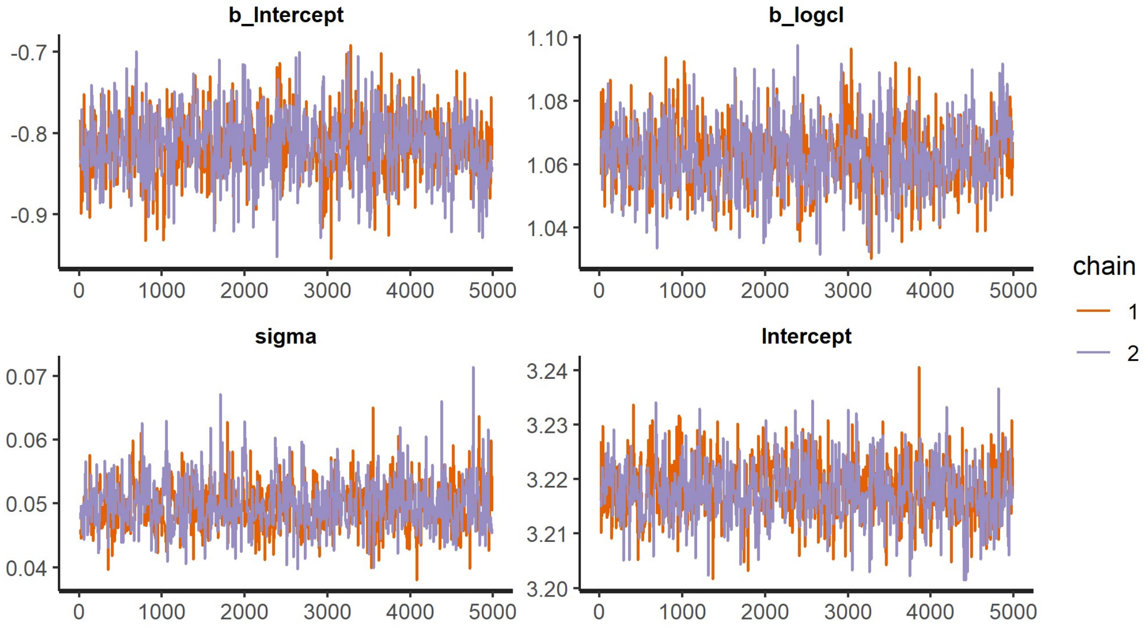

Figure B.2: MCMC trace plots for linear models estimating the carapace length-tail width relationship of juveniles in the Gisborne region (combined sex).

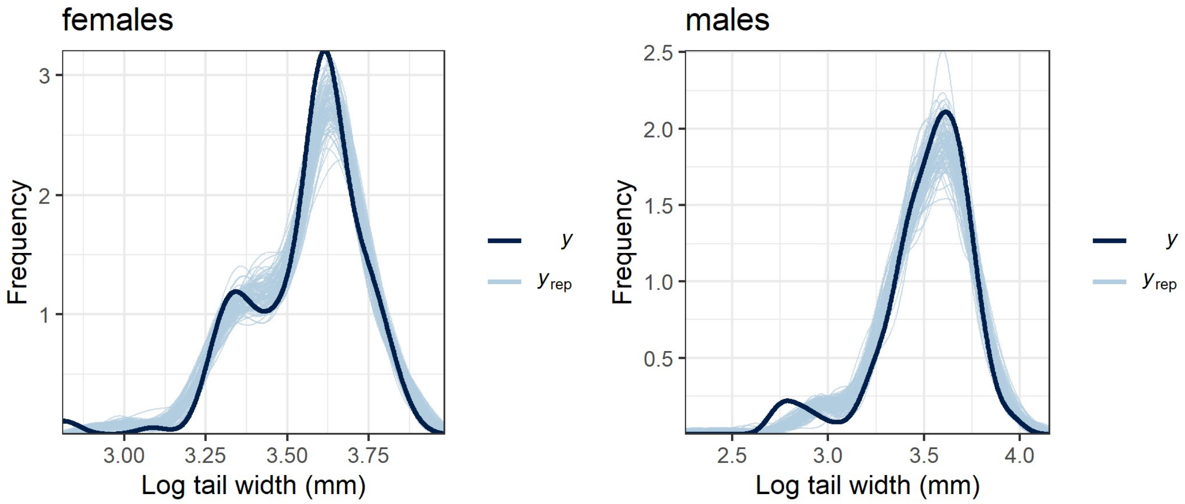

Figure B.3: Comparison of observed (black line) versus simulated (blue lines) density of log tail width of red rock lobsters from the posterior predictive distribution of the final linear models predicting the carapace length-tail width relationship of juveniles, using data collected at Halfmoon Bay, Stewart Island.

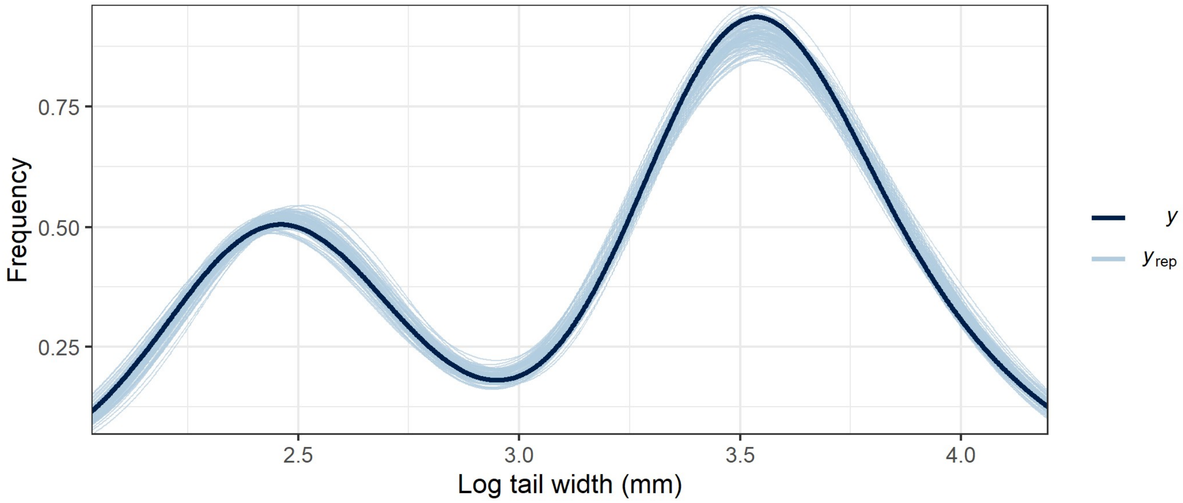

Figure B.4: Comparison of observed (black line) versus simulated (blue lines) density of log tail width from the posterior predictive distribution of the linear model predicting the carapace length-tail width relationship of juveniles, using data collected in the Gisborne region.

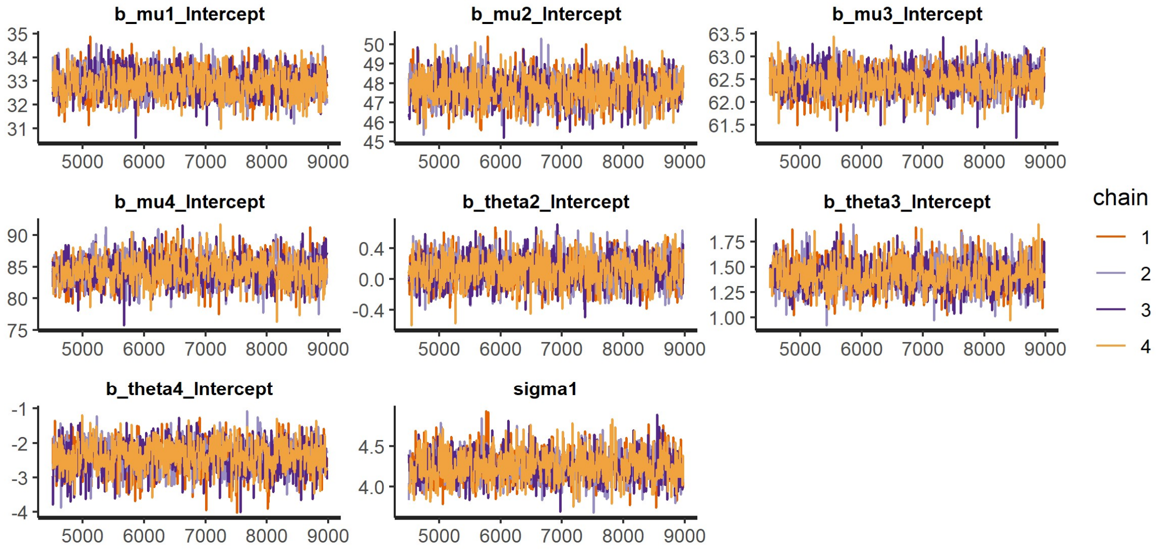

Figure B.5: Example MCMC trace plots from a mixture model specifying <u>four</u> mixture components (this model run was fitting to size composition data for males sampled at Halfmoon Bay, Stewart Island in 1984).

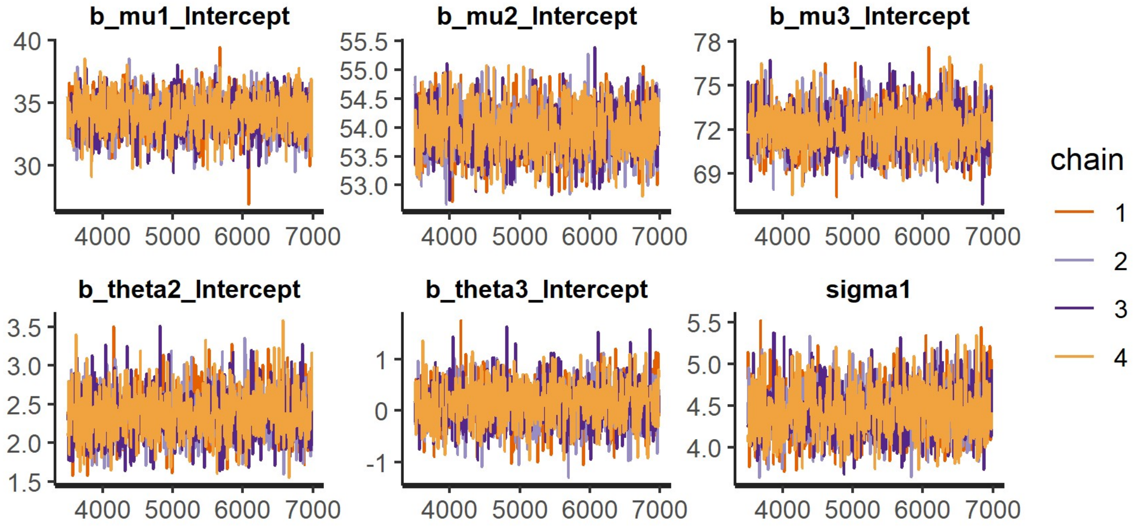

Figure B.6: Example MCMC trace plots from a mixture model specifying <u>three</u> mixture components (this model run was fitting to size composition data for females sampled at Halfmoon Bay, Stewart Island in 1982).

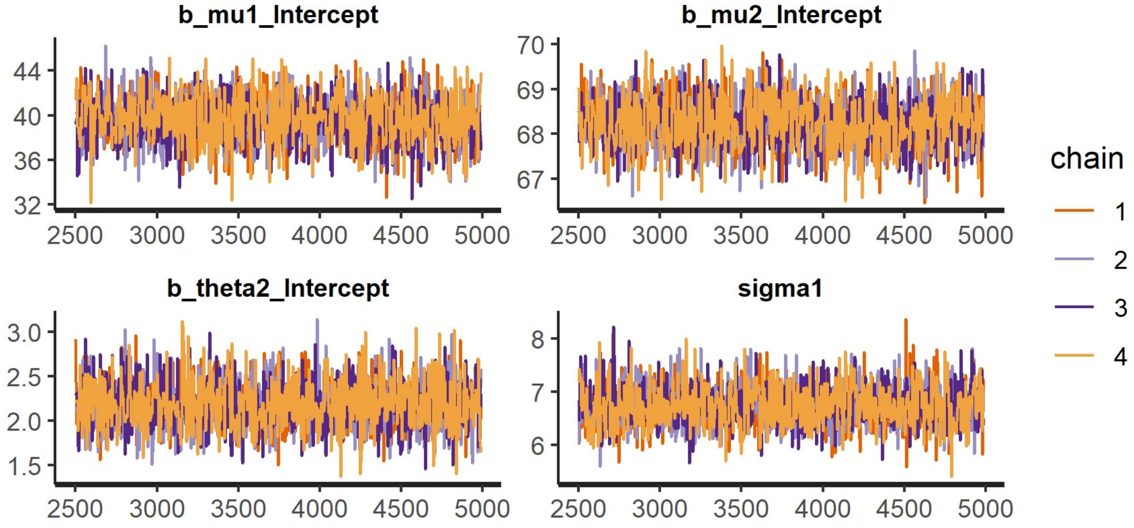

Figure B.7: Example MCMC trace plots from a mixture model specifying <u>two</u> mixture components (this model run was fitting to size composition data for males sampled at Halfmoon Bay, Stewart Island in 1987).

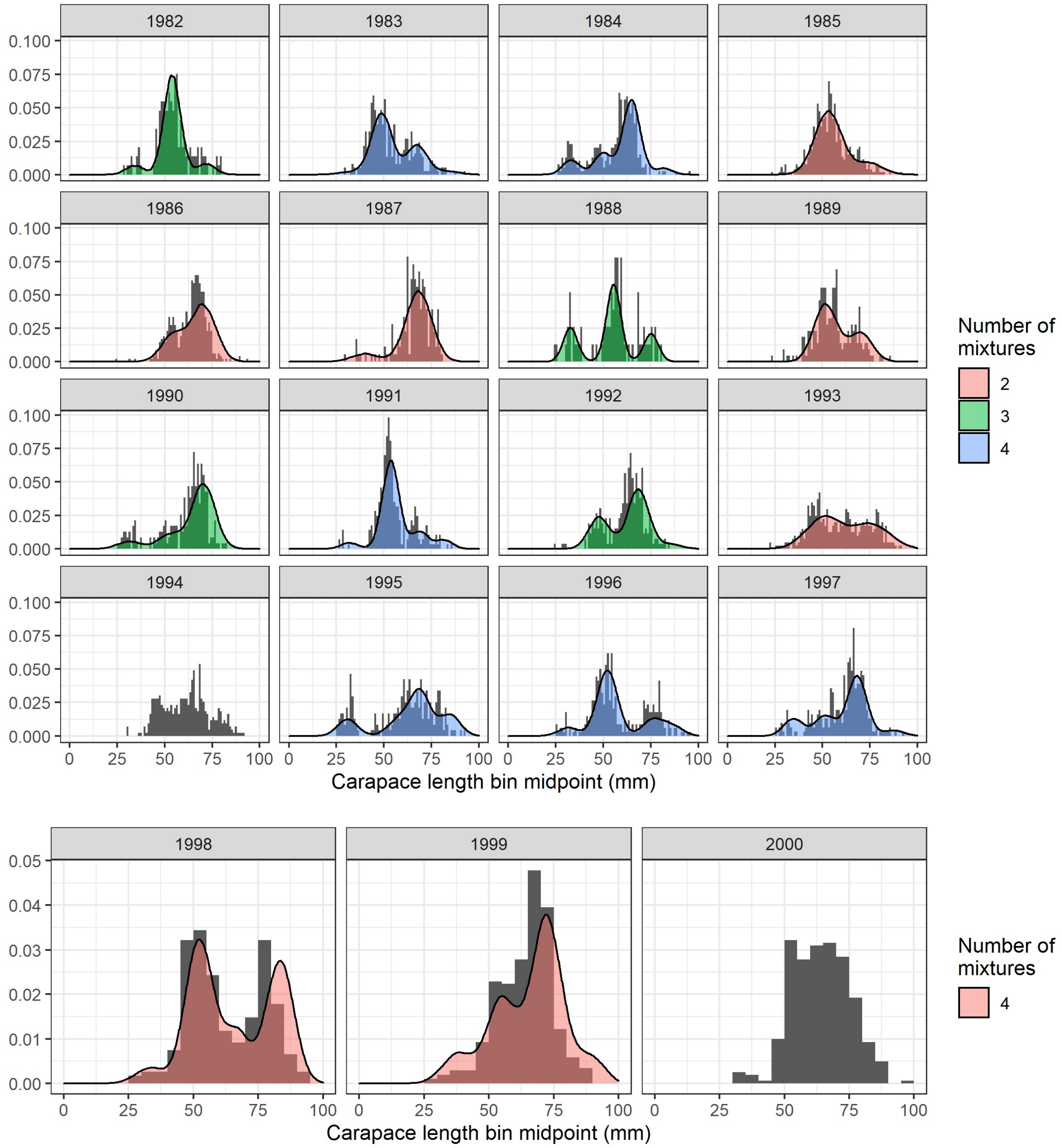

Figure B.8: **Observed length-frequency distribution (shaded bar plot) versus posterior predictive density (density plot) from mixture models fitted to size composition data of male juvenile red rock lobsters sampled at Halfmoon Bay, Stewart Island. Different colours for density plots indicate the number of mixture components in the optimal model for the respective year. No density plot is shown if an optimal model was not obtained for that year according to the chosen criterion.**

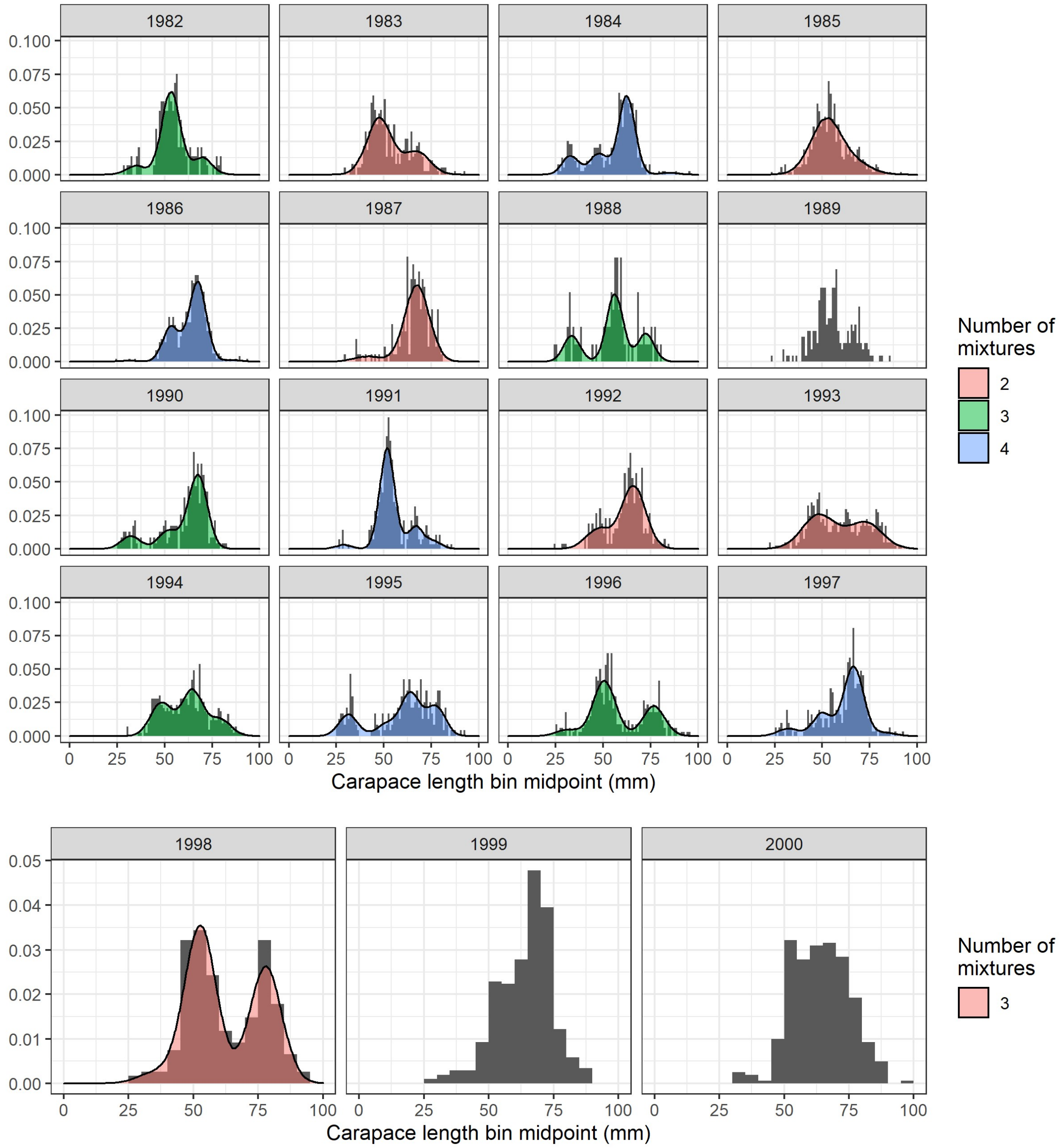

Figure B.9: **Observed length-frequency distribution (shaded bar plot) versus posterior predictive density (density plot) from mixture models fitted to size composition data of female juvenile red rock lobsters sampled at Halfmoon Bay, Stewart Island. Different colours for density plots indicate the number of mixture components in the optimal model for the respective year. No density plot is shown if an optimal model was not obtained for that year according to the chosen criterion.**

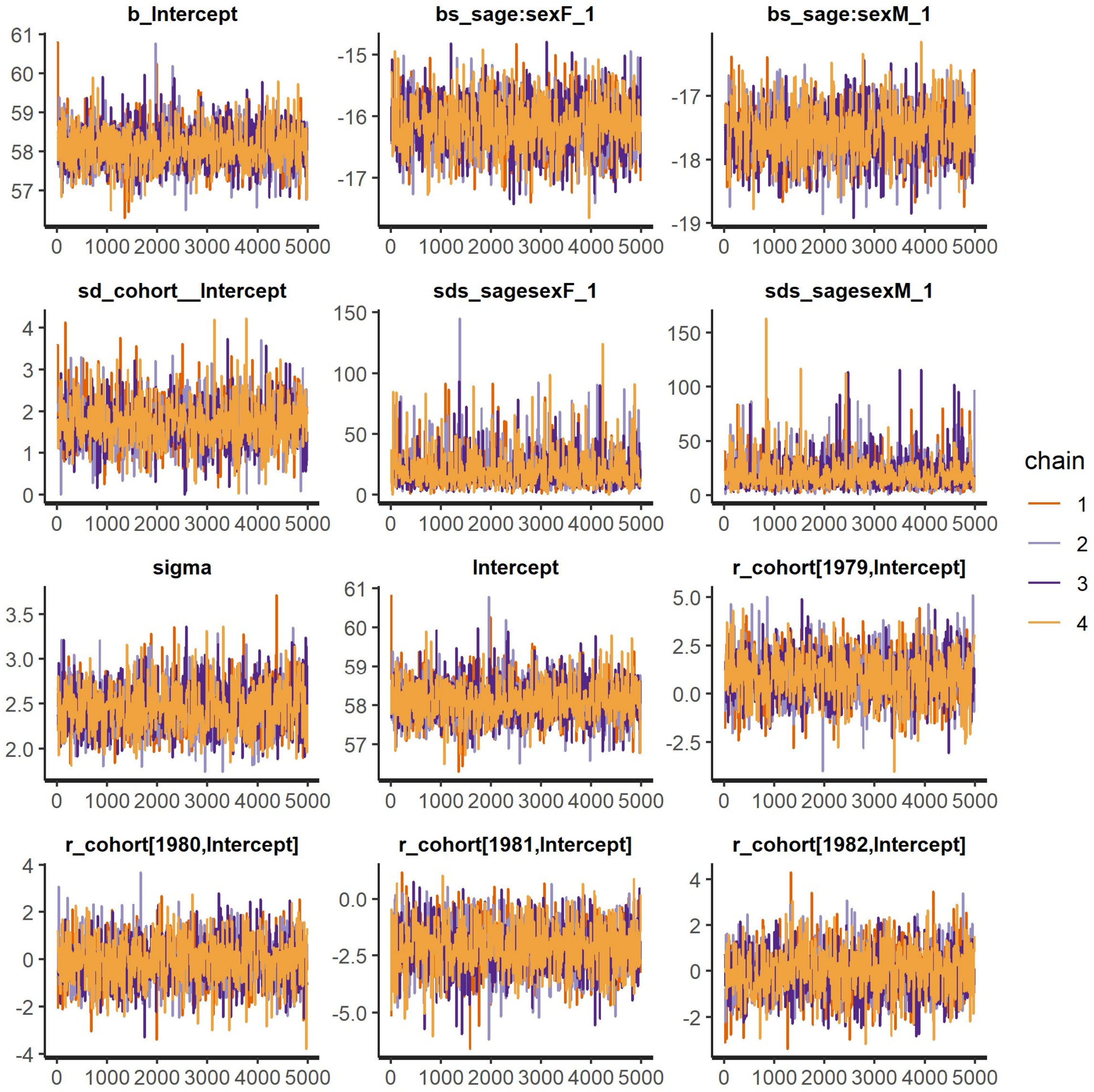

Figure B.10: MCMC trace plots for the final non-linear model estimating the growth rate of juvenile red rock lobster from the estimates of mixture models fitted to length-frequency data collected at Halfmoon Bay, Stewart Island (*lf_hm_7* from Table 2). This plot shows the traces of all the population effects and a sample of four levels of the group effect.

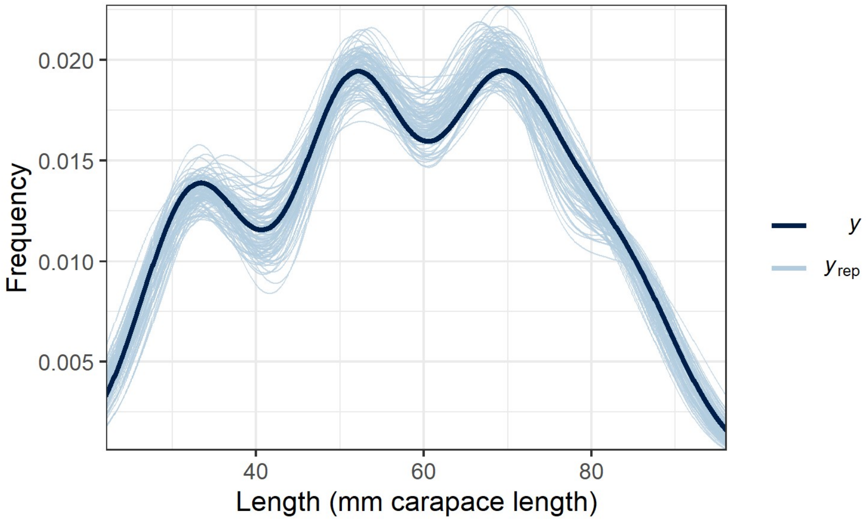

Figure B.11: **Comparison of observed (black line) versus simulated (blue lines) density of the mean carapace lengths of red rock lobster cohorts from the posterior predictive distribution of the final non-linear model estimating the growth rate of juvenile red rock lobster from the estimates of mixture models fitted to length-frequency data collected at Halfmoon Bay, Stewart Island (*lf_hm_7* from Table 2).**

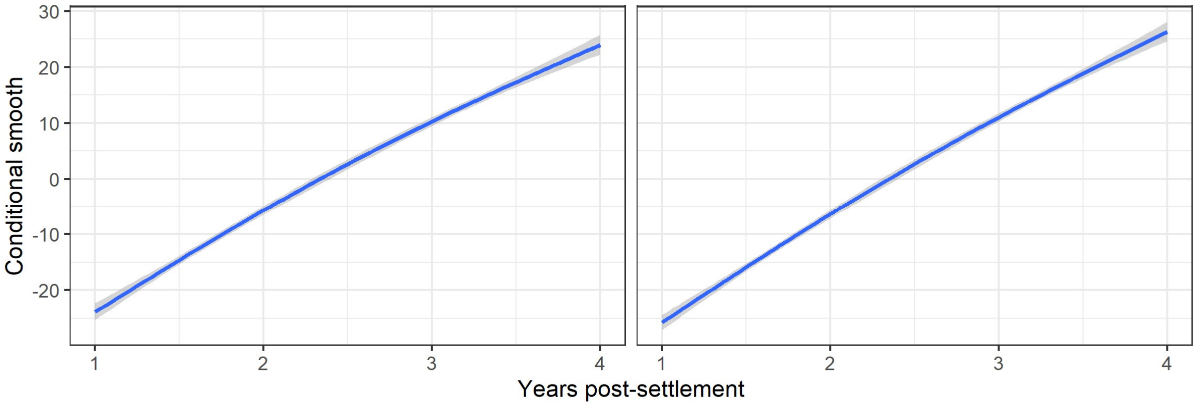

Figure B.12: **Conditional smoothers for the effect of years post-settlement as pueruli for males (left) and females (right) on the mean carapace length of red rock lobsters from the final non-linear model estimating the growth rate of juvenile red rock lobster from the estimates of mixture models fitted to length-frequency data collected at Halfmoon Bay, Stewart Island (*lf_hm_7* from Table 2). Blue lines represent medians and shaded areas represent the region of 95% credibility interval.**

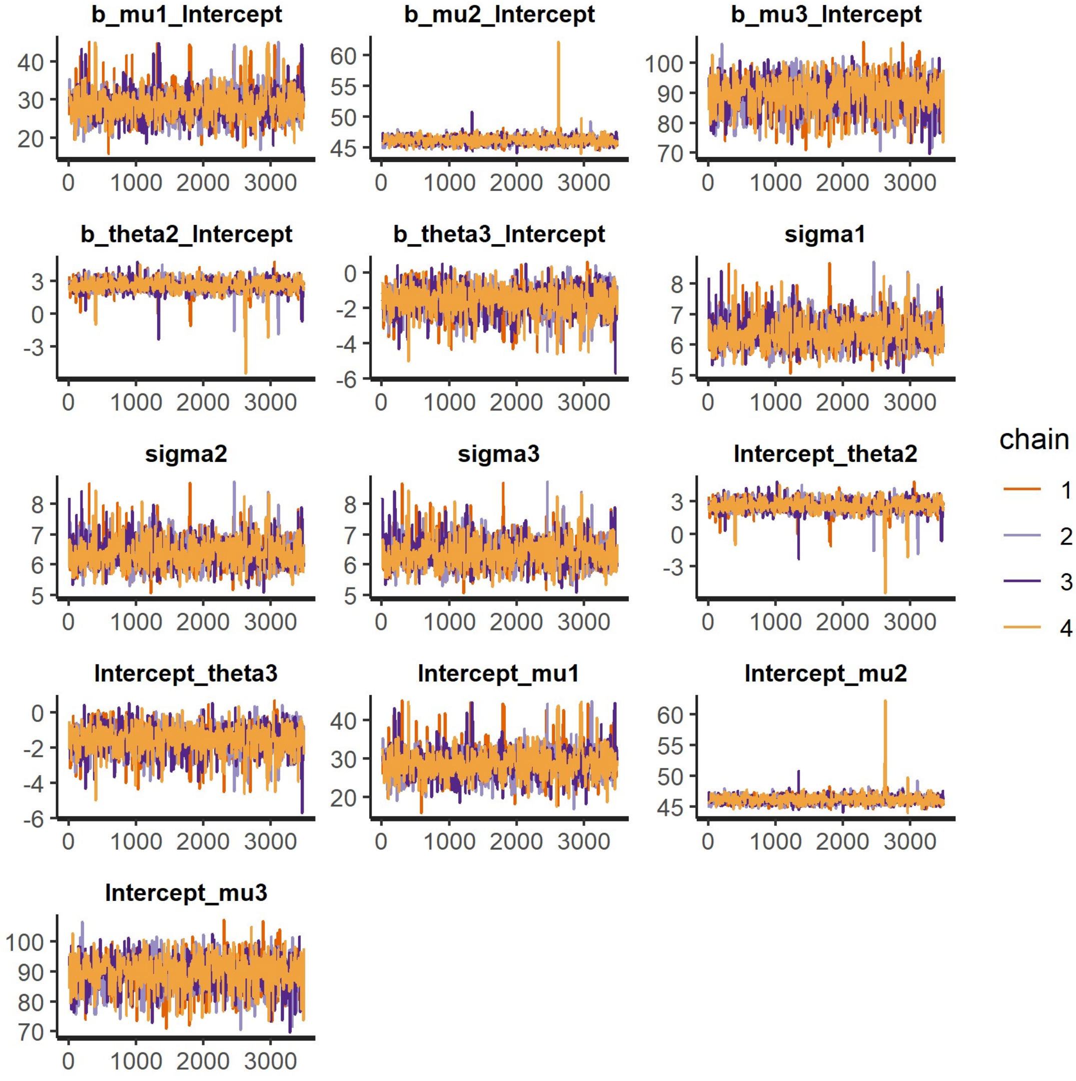

Figure B.13: Example MCMC trace plots from a mixture model specifying <u>three</u> mixture components (this model run was fitting to size composition data for males sampled at Gisborne Wharf in March 1977).

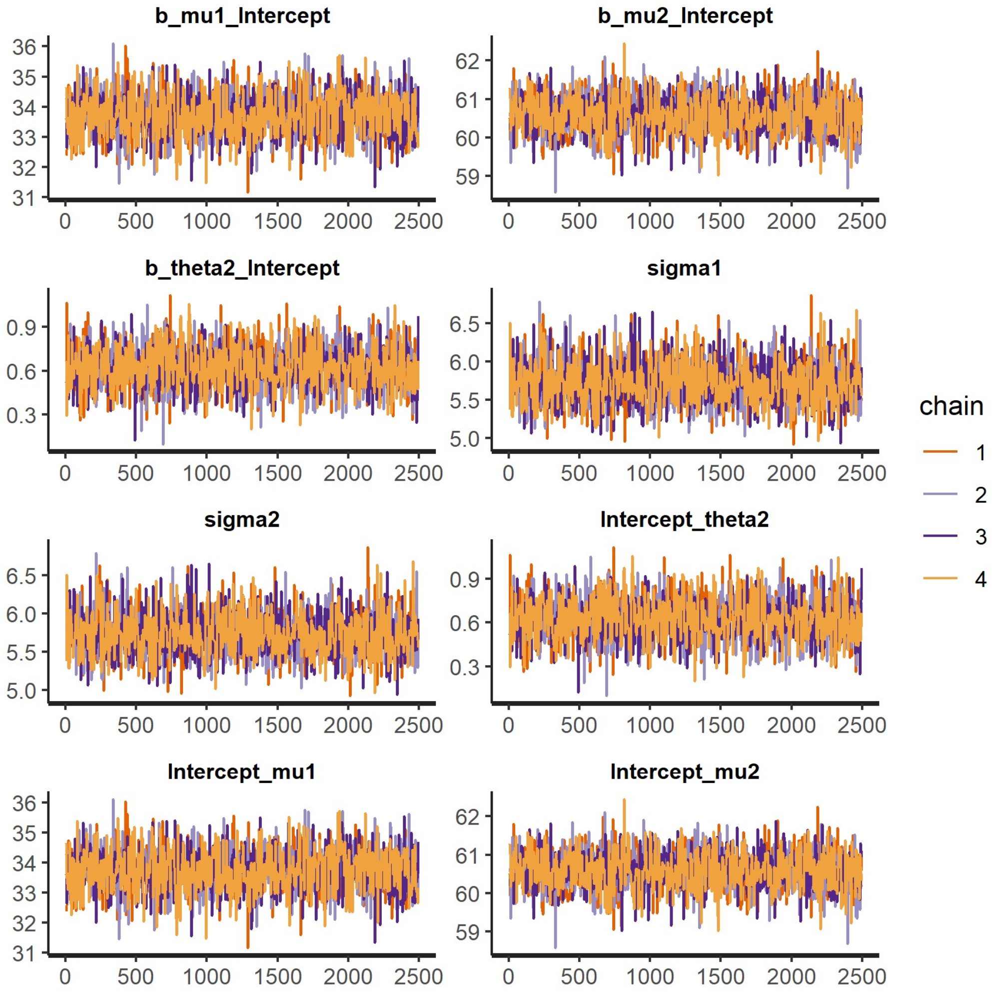

Figure B.14: Example MCMC trace plots from a mixture model specifying two mixture components (this model run was fitting to size composition data for males sampled at Gisborne Wharf in February 1976).

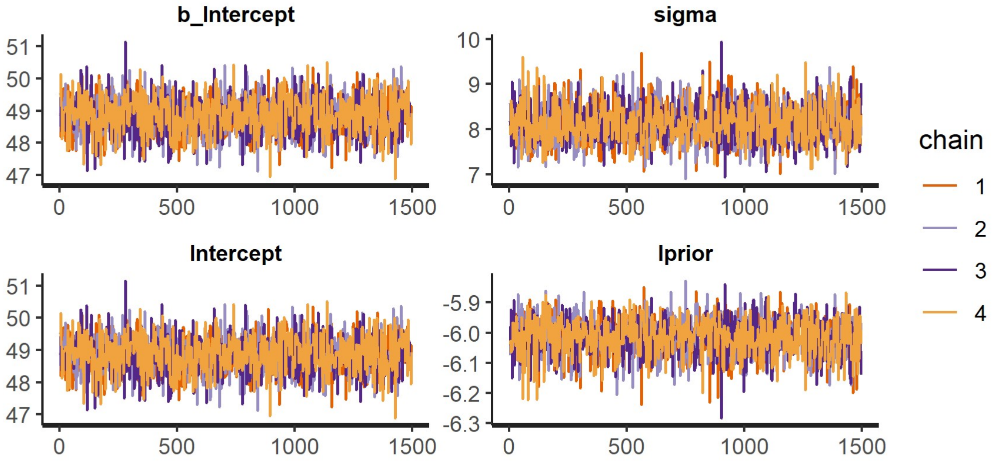

Figure B.15: Example MCMC trace plots from a mixture model specifying one mixture component (this model run was fitting to size composition data for males sampled at Gisborne Wharf in October 1976).

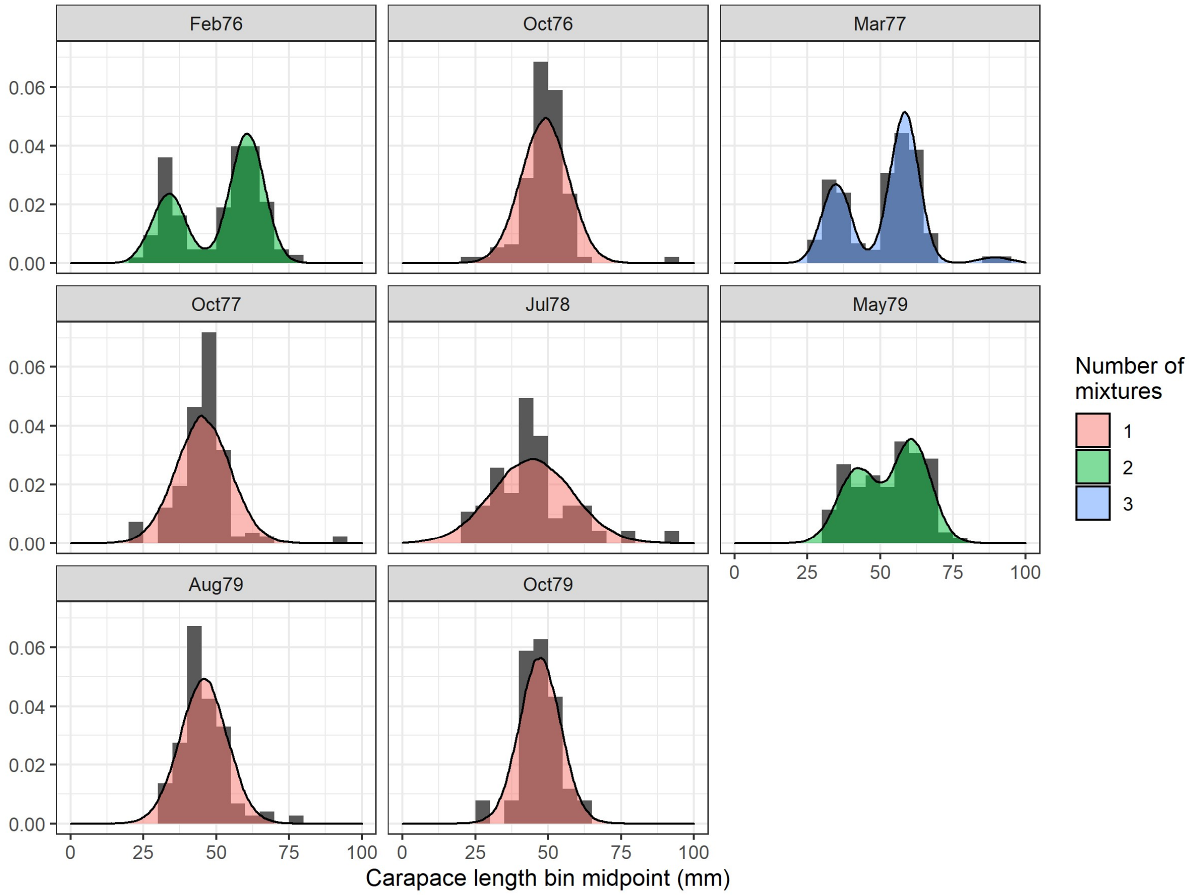

Figure B.16: Observed length-frequency distribution (shaded bar plot) versus posterior predictive density (density plot) from mixture models fitted to size composition data of unsexed juvenile red rock lobsters sampled at Gisborne Wharf. Different colours for density plots indicate the number of mixture components in the optimal model for the respective year. No density plot is shown if an optimal model was not obtained for that year according to the chosen criterion.

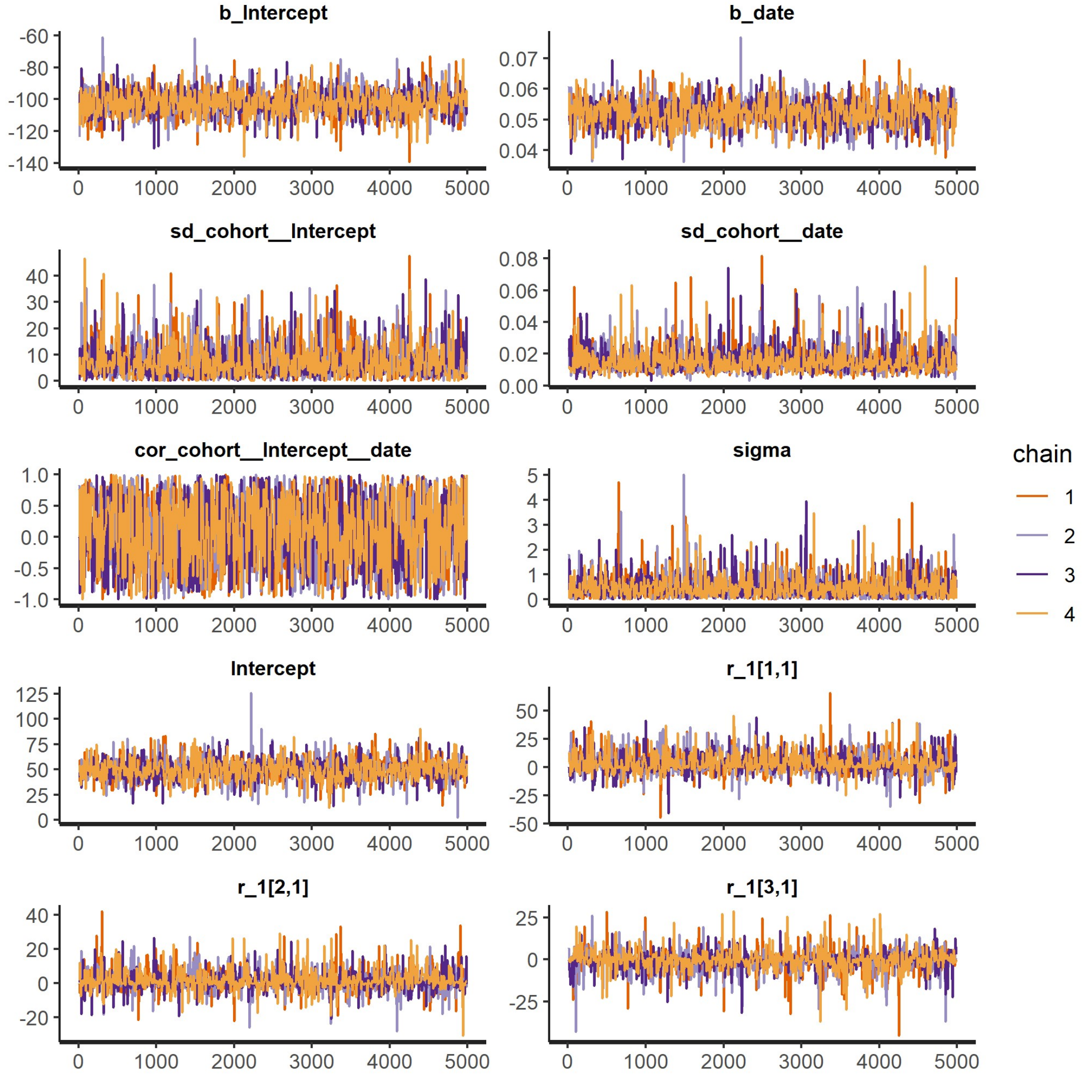

Figure B.17: **MCMC trace plots for the final model for estimating the growth rate of juvenile red rock lobsters from the estimates of mixture models fitted to length-frequency data collected at Gisborne Wharf (*lf_gw_4* from Table 5). This plot shows the traces of all the population effects and a sample of three levels of the group effect.**

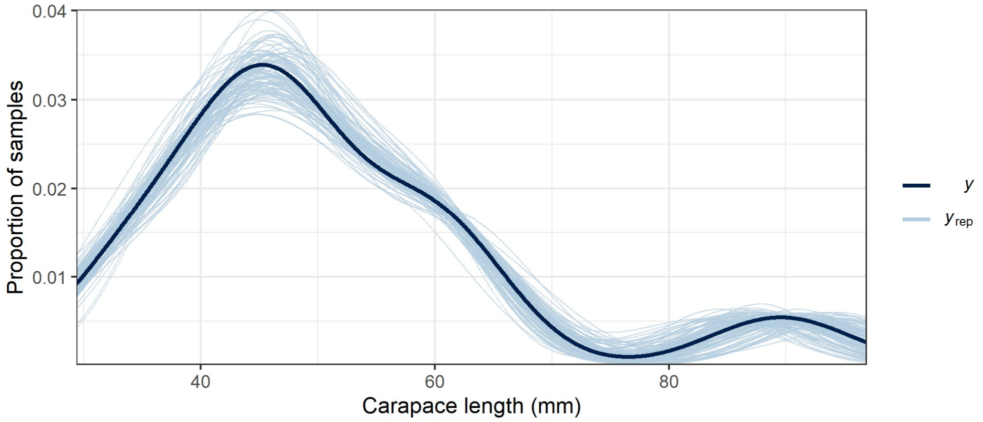

Figure B.18: **Comparison of observed (black line) versus simulated (blue lines) density of the mean carapace lengths of red rock lobster cohorts from the posterior predictive distribution of the final model estimating growth rate at Gisborne Wharf (*lf_gw_4* from Table 5).**

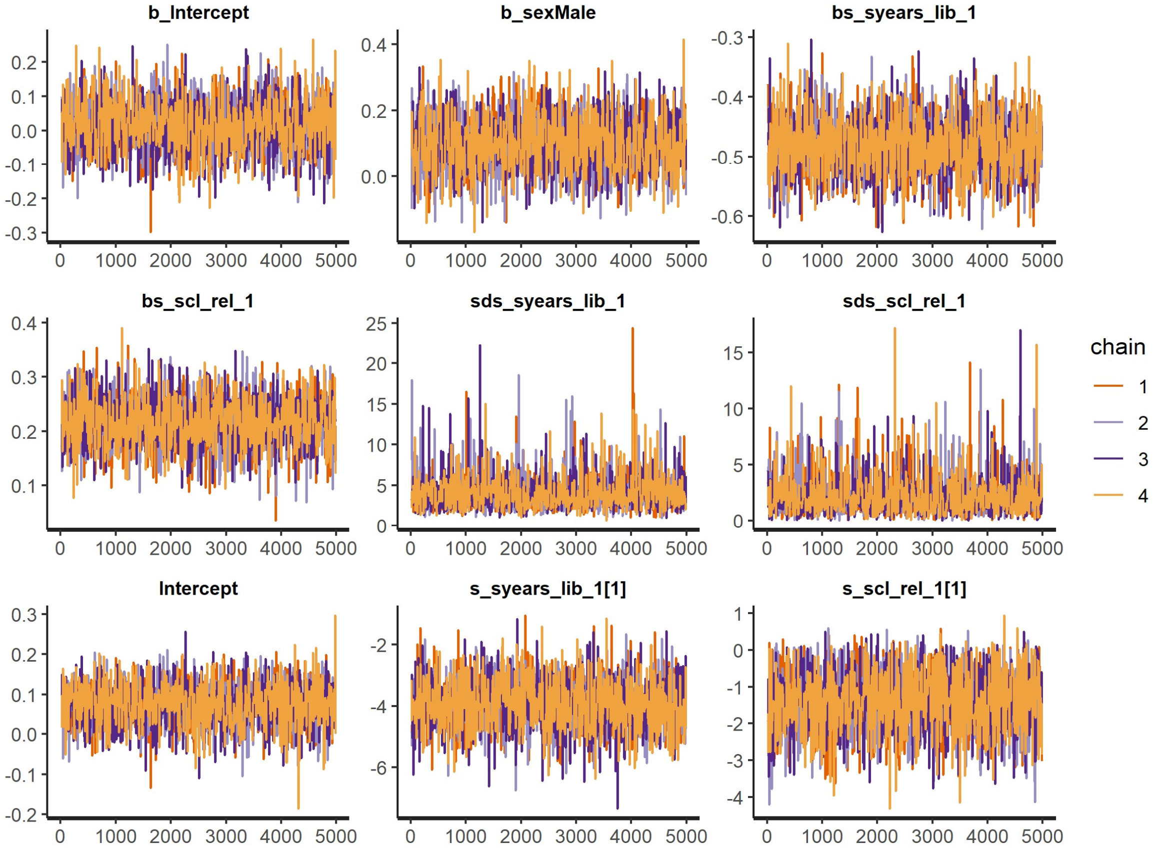

Figure B.19: **MCMC trace plots for the selected model for estimating the growth rate of juvenile red rock lobster from mark-recapture size increment data collected at Halfmoon Bay, Stewart Island (model *tag9* from Table 4).**

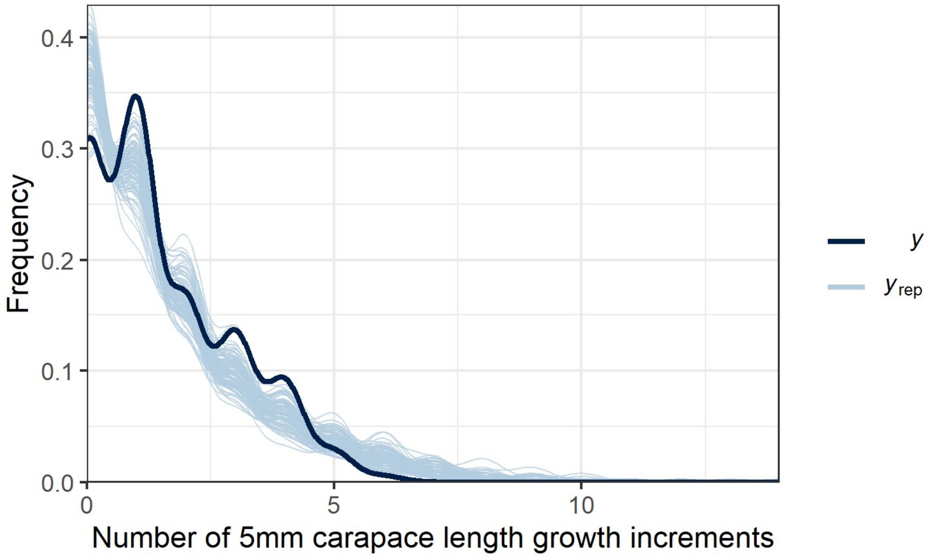

Figure B.20: **Comparison of observed (black line) versus simulated (blue lines) density of CL growth increments of red rock lobsters from the posterior predictive distribution of the final model for predicting the growth rate of juvenile red rock lobster from mark-recapture size increment data collected at Halfmoon Bay, Stewart Island (model *tag9* from Table 4).**

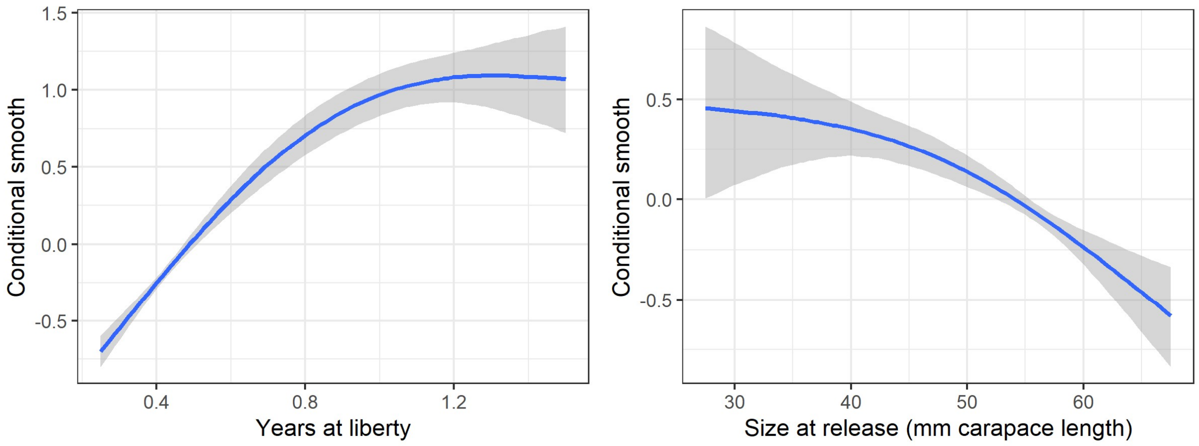

Figure B.21: Conditional smooths for the effects of years-at-liberty (left) and size-at-release (right) on the growth increment in carapace length of red rock lobsters from the final model for predicting the growth rate of juvenile red rock lobster from mark-recapture size increment data collected at Halfmoon Bay, Stewart Island (model *tag9* from Table 4). Blue lines represent medians and shaded areas represent the region of 95% probability.

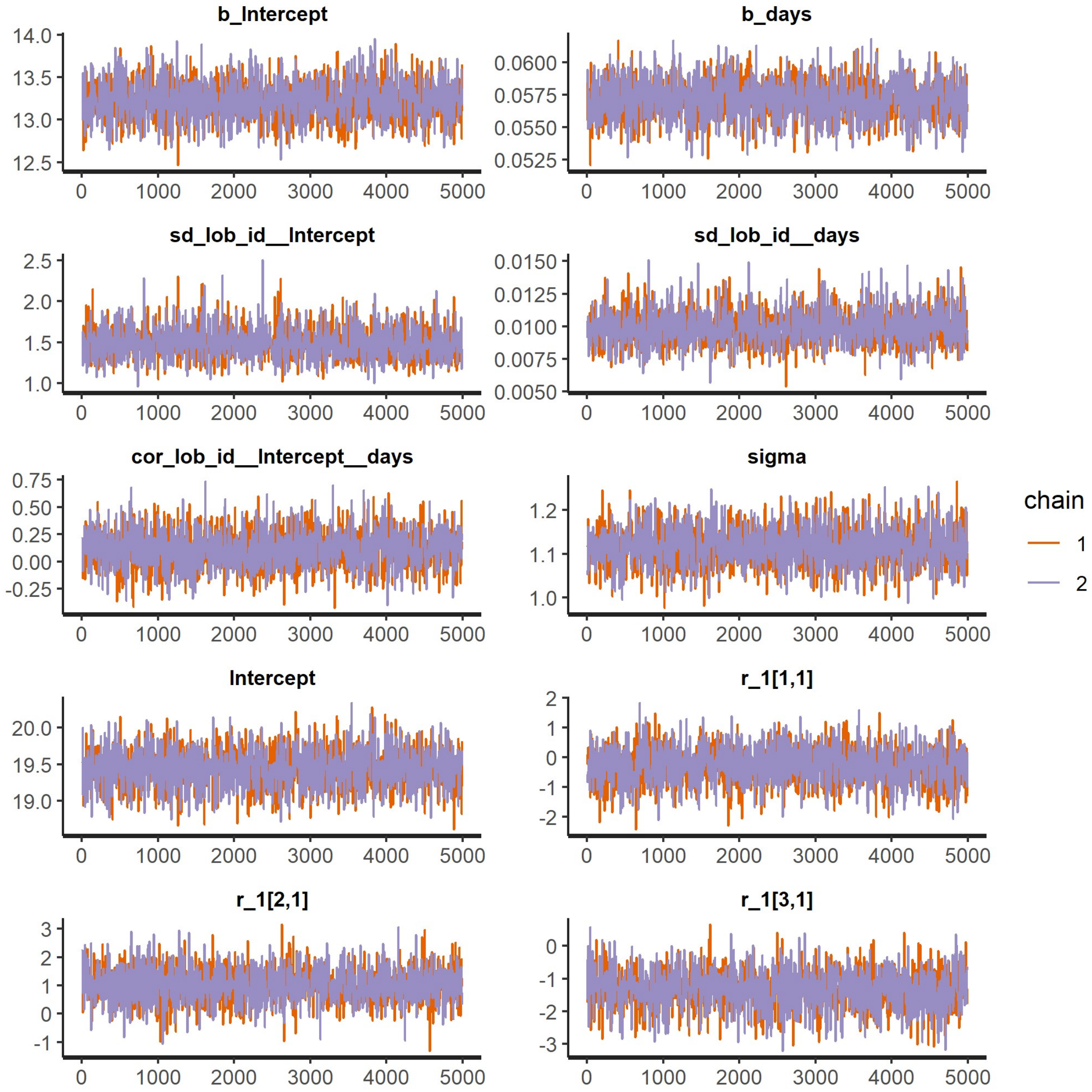

Figure B.22: MCMC trace plots for model *mah4* for predicting the growth rate of captive lobsters (model *mah4* from Table 8). This plot shows all population level effect traces and a sample of three group level effect traces (the remainder all demonstrated good mixing).

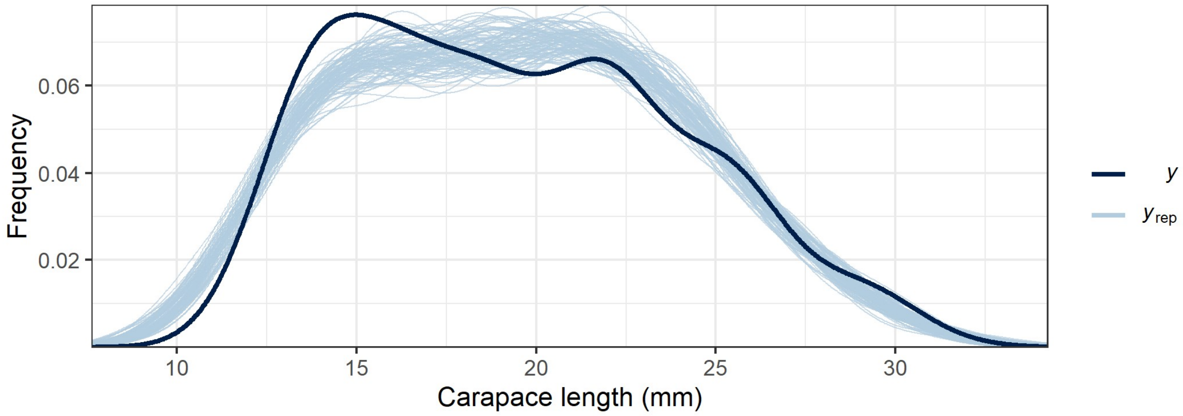

Figure B.23: Comparison of observed (black line) versus simulated (blue lines) density of carapace length measurements of post-settlement captive lobsters from the posterior predictive distribution of the optimal linear model for predicting the growth rate of captive lobsters (*mah4* from Table 8).

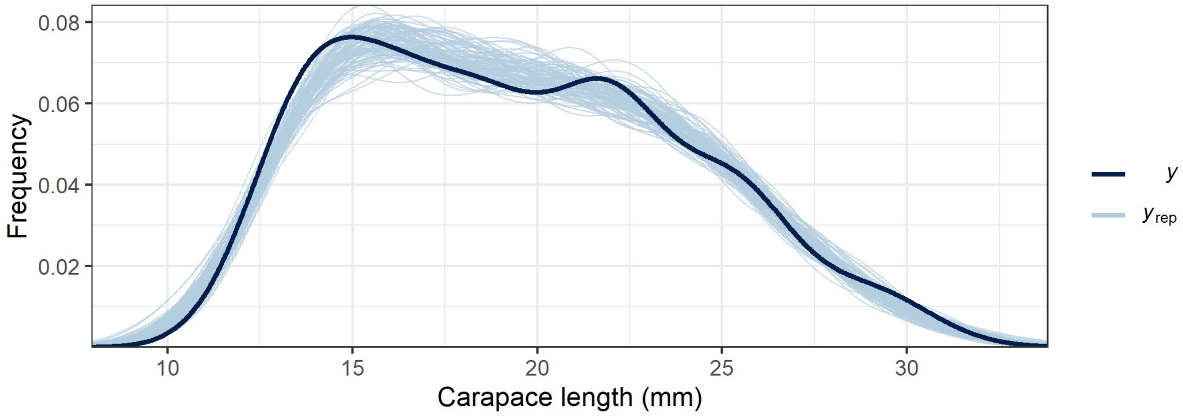

Figure B.24: **Comparison of observed (black line) versus simulated (blue lines) density of carapace length measurements of post-settlement captive lobsters from the posterior predictive distribution of the optimal <u>non-linear model</u> for predicting the growth rate of captive lobsters (*mah5* from Table 8).**

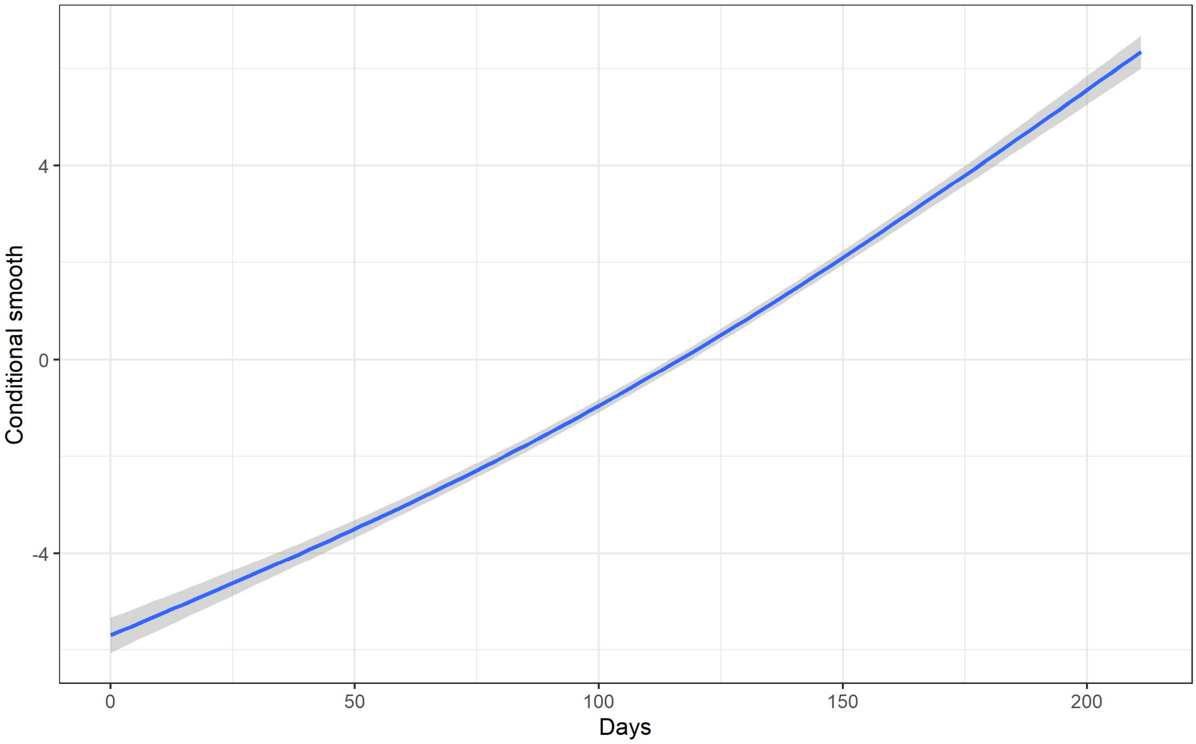

Figure B.25: **Conditional smooth for the effects of day on the size in the carapace length of red rock lobsters the optimal <u>non-linear model</u> for predicting the growth rate of captive lobsters (*mah5* from Table 8). Blue lines represent medians and shaded areas represent the region of 95% probability.**

APPENDIX C. PARAMETER ESTIMATES

Table C.1: Parameter estimates of model for predicting tail width (TW) from carapace length (CL) (Equation 1) <u>for males</u> using data from diver surveys at <u>Halfmoon Bay, Stewart Island</u> (model *tw_m*).

Parameter	Parameter label	Mean	SD	2.5%	Median	97.5%
α	b_Intercept	3.513	0.005	3.503	3.513	3.524
β	b_logcl	0.985	0.024	0.938	0.985	1.029
σ	sigma	0.070	0.004	0.063	0.070	0.078

Table C.2: Parameter estimates of model for predicting tail width (TW) from carapace length (CL) (Equation 1) <u>for females</u> using data from diver surveys at <u>Halfmoon Bay, Stewart Island</u> (model *tw_f*).

Parameter	Parameter label	Mean	SD	2.5%	Median	97.5%
α	b_Intercept	3.558	0.004	3.550	3.558	3.564
β	b_logcl	1.018	0.021	0.975	1.019	1.060
σ	sigma	0.044	0.002	0.040	0.044	0.050

Table C.3: Parameter estimates of model for predicting tail width (TW) from carapace length (CL) (Equation 1) <u>for both sexes</u> using data from diver surveys in the <u>Gisborne region</u> (model *tw_gis*).

Parameter	Parameter label	Mean	SD	2.5%	Median	97.5%
α	b_Intercept	3.218	0.006	3.206	3.218	3.230
β	b_logcl	1.063	0.011	1.041	1.062	1.086
σ	sigma	0.050	0.004	0.042	0.050	0.059

Table C.4: Parameter estimates of mixture models (Equation 2) fitted to length frequencies of <u>males</u> from diver surveys at Halfmoon Bay, Stewart Island. Mean value with 95% credible interval in parentheses.

Year	μ_1	μ_2	μ_3	μ_4	θ_2	θ_3	θ_4	σ
1982	34.00 (30.92–36.93)	53.94 (53.11–54.78)	72.04 (69.33–75.03)	–	2.36 (1.78–3.02)	0.13 (-0.67–0.93)	–	4.42 (3.88–5.09)
1983	31.12 (25.84–36.42)	48.70 (47.84–49.55)	67.41 (65.96–68.93)	84.51 (80.08–89.47)	3.16 (2.44–3.99)	2.43 (1.67–3.27)	0.20 (-0.82–1.23)	5.35 (4.85–5.97)
1984	33.01 (31.73–34.34)	49.93 (48.59–51.26)	64.86 (64.22–65.47)	81.66 (79.36–84.10)	0.43 (0.06–0.80)	1.65 (1.37–1.99)	-0.84 (-1.40–-0.31)	4.40 (4.03–4.83)
1985	–	52.03 (50.75–53.50)	68.44 (63.61–72.95)	–	-1.80 (-2.73–-1.11)	–	–	8.23 (7.39–9.32)
1986	–	54.64 (53.15–56.18)	70.58 (69.54–71.51)	–	0.76 (0.48–1.05)	–	–	6.41 (5.81–7.24)
1987	39.57 (35.19–43.81)	–	68.24 (67.13–69.34)	–	2.18 (1.67–2.74)	–	–	6.75 (6.02–7.57)
1988	32.75 (30.97–34.51)	55.49 (54.33–56.67)	75.17 (73.23–77.16)	–	0.83 (0.30–1.39)	-0.20 (-0.88–0.46)	–	3.67 (3.10–4.38)
1989	–	51.58 (50.45–52.84)	70.17 (68.24–72.07)	–	-0.71 (-1.06–-0.37)	–	–	6.10 (5.37–7.01)
1990	31.61 (28.17–35.41)	52.93 (49.53–56.66)	70.41 (69.20–71.49)	–	0.61 (-0.09–1.28)	2.14 (1.67–2.67)	–	6.06 (5.31–7.05)
1991	31.72 (29.26–34.17)	53.48 (52.88–54.08)	68.73 (66.78–70.70)	81.73 (79.44–83.83)	2.67 (2.22–3.19)	1.04 (0.48–1.64)	0.36 (-0.26–1.00)	4.40 (4.00–4.85)
1992	–	47.87 (46.67–49.08)	68.43 (67.44–69.38)	85.53 (81.10–89.79)	0.64 (0.37–0.91)	-1.93 (-2.7–-1.25)	–	5.44 (4.94–6.05)
1993	–	51.16 (49.50–52.90)	76.29 (74.29–78.24)	–	-0.28 (-0.56–-0.01)	–	–	9.43 (8.62–10.37)
1994	–	–	–	–	–	–	–	–
1995	30.87 (29.35–32.37)	57.12 (53.37–61.44)	68.91 (66.93–71.45)	84.77 (82.67–86.79)	-0.08 (-0.83–0.63)	0.99 (0.52–1.36)	0.23 (-0.23–0.67)	5.25 (4.59–6.18)
1996	31.34 (29.31–33.39)	31.34 (29.31–33.39)	31.34 (29.31–33.39)	31.34 (29.31–33.39)	2.08 (1.72–2.47)	0.64 (-0.01–1.19)	0.17 (-0.59–0.90)	5.14 (4.72–5.62)
1997	34.54 (33.19–36.00)	51.30 (49.58–53.00)	68.14 (67.37–68.93)	87.63 (84.9–90.20)	0.14 (-0.25–0.51)	1.25 (0.96–1.53)	-1.14 (-1.72–-0.63)	5.00 (4.58–5.51)
1998	–	52.40 (51.28–53.46)	–	80.98 (79.66–82.22)	-0.23 (-0.42–-0.04)	–	–	8.05 (7.49–8.64)
1999	–	48.82 (44.98–52.69)	71.46 (69.35–73.42)	–	1.07 (0.61–1.61)	–	–	10.39 (9.24–11.83)
2000	–	–	–	–	–	–	–	–

Table C.5: Parameter estimates of mixture models (Equation 2) fitted to length frequencies of <u>females</u> from diver surveys at Halfmoon Bay, Stewart Island. Mean value with 95% credible interval in parentheses.

Year	μ_1	μ_2	μ_3	μ_4	θ_2	θ_3	θ_4	σ
1982	34.83 (31.56–38.52)	53.26 (52.22–54.45)	70.10 (67.51–72.83)	–	2.21 (1.61–2.89)	0.62 (-0.14–1.42)	–	4.89 (4.17–5.90)
1983	–	47.63 (46.57–48.77)	67.46 (65.85–69.16)	–	-0.90 (-1.22–-0.63)	–	–	6.65 (6.05–7.40)
1984	32.91 (31.81–34.10)	47.72 (46.19–49.20)	62.48 (61.89–63.05)	84.49 (80.10–88.89)	0.11 (-0.27–0.50)	1.42 (1.14–1.73)	-2.39 (-3.39–-1.54)	4.25 (3.90–4.64)
1985	–	52.03 (50.75–53.50)	68.44 (63.61–72.95)	–	-1.80 (-2.73–-1.11)	–	–	8.23 (7.39–9.32)
1986	31.16 (25.76–37.31)	53.36 (52.39–54.31)	67.38 (66.79–67.97)	85.92 (81.50–90.59)	3.38 (2.56–4.31)	4.21 (3.42–5.14)	0.32 (-0.88–1.54)	4.46 (4.10–4.88)
1987	40.97 (36.05–45.84)	–	67.46 (66.46–68.47)	–	2.64 (2.03–3.35)	–	–	6.43 (5.76–7.16)
1988	33.49 (31.32–35.73)	56.16 (54.76–57.53)	72.63 (70.42–74.85)	–	0.95 (0.40–1.52)	0.03 (-0.66–0.68)	–	4.22 (3.54–5.14)
1989	–	–	–	–	–	–	–	–
1990	32.10 (30.07–34.09)	51.90 (49.78–54.10)	67.33 (66.42–68.24)	–	0.37 (-0.16–0.91)	1.76 (1.35–2.17)	–	4.92 (4.39–5.56)
1991	28.73 (25.93–31.72)	51.71 (51.14–52.30)	66.39 (64.25–68.35)	76.72 (73.02–80.19)	3.20 (2.58–3.97)	1.72 (1.00–2.58)	0.58 (-0.47–1.69)	3.95 (3.56–4.44)
1992	–	47.15 (44.99–49.33)	65.94 (64.84–67.02)	–	1.18 (0.83–1.56)	–	–	6.41 (5.69–7.31)
1993	–	48.09 (46.43–49.71)	72.53 (70.74–74.41)	–	-0.25 (-0.51–0.02)	2.14 (1.62–2.74)	1.19 (0.62–1.82)	8.71 (7.97–9.60)
1994	–	48.04 (46.82–49.37)	64.57 (63.36–65.83)	79.55 (77.56–81.43)	0.32 (0.06–0.59)	-0.73 (-1.13–-0.36)	–	5.53 (4.97–6.22)
1995	31.37 (29.88–32.96)	51.39 (47.81–56.18)	64.07 (61.89–66.34)	77.46 (75.47–79.32)	-0.57 (-1.31–0.10)	0.68 (0.26–1.06)	0.31 (-0.14–0.75)	4.76 (4.11–5.81)
1996	31.17 (28.31–34.23)	50.70 (49.83–51.54)	–	76.77 (75.69–77.87)	2.20 (1.72–2.67)	1.57 (1.08–2.08)	–	5.66 (5.21–6.18)
1997	31.84 (29.30–34.59)	50.19 (48.46–51.99)	66.52 (65.62–67.38)	83.17 (78.65–87.83)	1.08 (0.52–1.62)	2.18 (1.74–2.68)	-0.85 (-1.79–-0.02)	5.05 (4.49–5.76)
1998	34.46 (29.83–39.52)	52.63 (51.75–53.55)	–	77.84 (76.89–78.79)	2.70 (2.02–3.43)	2.40 (1.72–3.12)	–	6.07 (5.62–6.58)
1999	–	–	–	–	–	–	–	–
2000	–	–	–	–	–	–	–	–

Table C.6: Parameter estimates from the selected model (Equation 3, Equation 4) for estimating the growth rate of juvenile red rock lobster from length-based growth information at Halfmoon Bay, Stewart Island (model *lf_hm_7* from Table 2).

Parameter	Parameter label	Mean	SD	2.5%	Median	97.5%
β_0	b_Intercept	58.115	0.511	57.155	58.110	59.212
–	bs_sage:sexF_1	-16.154	0.421	-16.985	-16.163	-15.312
–	bs_sage:sexM_1	-17.586	0.407	-18.387	-17.593	-16.770
–	s_sagesexF_1[1]	-11.469	4.518	-19.588	-11.451	-2.451
–	s_sagesexM_1[1]	-10.417	4.250	-18.573	-10.539	-1.678
–	sds_sagesexF_1	20.047	10.108	3.454	16.150	64.590
–	sds_sagesexM_1	19.230	9.897	3.491	15.248	56.768
μ_h	r_cohort[1979,Intercept]	0.846	1.185	-1.532	0.777	3.364
μ_h	r_cohort[1980,Intercept]	-0.067	0.963	-1.982	-0.073	1.806
μ_h	r_cohort[1981,Intercept]	-2.138	1.152	-4.306	-2.161	-0.015
μ_h	r_cohort[1982,Intercept]	-0.012	1.022	-2.027	-0.013	2.039
μ_h	r_cohort[1983,Intercept]	0.062	0.926	-1.883	0.050	1.991
μ_h	r_cohort[1984,Intercept]	0.262	0.992	-1.705	0.236	2.323
μ_h	r_cohort[1985,Intercept]	1.762	1.352	-0.761	1.694	4.582
μ_h	r_cohort[1986,Intercept]	2.462	1.220	0.060	2.477	5.031
μ_h	r_cohort[1987,Intercept]	-0.725	0.958	-2.659	-0.700	1.094
μ_h	r_cohort[1988,Intercept]	-0.162	0.992	-2.394	-0.139	1.942
μ_h	r_cohort[1989,Intercept]	-0.590	0.900	-2.553	-0.551	1.224
μ_h	r_cohort[1990,Intercept]	-0.576	0.906	-2.475	-0.553	1.268
μ_h	r_cohort[1991,Intercept]	-1.757	1.113	-3.993	-1.724	0.307
μ_h	r_cohort[1992,Intercept]	-1.748	1.124	-4.078	-1.671	0.350
μ_h	r_cohort[1993,Intercept]	1.848	1.203	-0.327	1.827	4.272
μ_h	r_cohort[1994,Intercept]	-1.285	0.907	-3.194	-1.266	0.457
μ_h	r_cohort[1995,Intercept]	-0.756	0.983	-2.807	-0.697	1.116
μ_h	r_cohort[1996,Intercept]	0.450	0.910	-1.553	0.431	2.486
μ_h	r_cohort[1997,Intercept]	0.733	1.220	-1.531	0.690	3.326
μ_h	r_cohort[1998,Intercept]	1.409	1.502	-1.532	1.299	5.016
σ^h	sd_cohort__Intercept	1.714	0.496	0.633	1.668	2.858
σ	sigma	2.452	0.253	1.987	2.433	3.004

Table C.7: Parameter estimates of mixture models (Equation 2) fitted to length frequencies of unsexed lobsters from diver surveys at Gisborne Wharf. Mean value with 95% credible interval in parentheses.

Month-Year	μ_1	μ_2	μ_3	θ_2	θ_3	σ
Feb-1976	33.72 (32.34–35.14)	60.59 (59.58–61.54)	–	0.63 (0.33–0.92)	–	5.74 (5.20–6.34)
Oct-1976	48.85 (47.68–49.97)	–	–	–	–	8.12 (7.35–9.02)
Mar-1977	28.88 (21.38–38.20)	46.21 (45.00–47.46)	89.53 (77.16–99.20)	2.57 (1.50–3.70)	-1.58 (-3.36–-0.14)	6.39 (5.55–7.46)
Oct-1977	44.62 (41.78–47.40)	–	–	–	–	13.86 (12.08–15.94)
Jul-1978	51.08 (49.09–53.19)	–	–	–	–	13.50 (12.14–15.05)
May-1979	39.12 (25.37–47.10)	46.76 (40.92–50.30)	52.07 (46.81–62.80)	0.94 (-3.09–4.05)	0.13 (-3.59–3.81)	6.25 (4.31–8.18)
Aug-1979	53.04 (50.72–55.38)	–	–	–	–	11.64 (10.16–13.47)
Oct-1979	45.57 (44.22–46.91)	–	–	–	–	8.13 (7.21–9.17)

Table C.8: Parameter estimates from the selected model (Equation 3, Equation 5) for estimating the growth rate of juvenile red rock lobster from length-based growth information at Gisborne Wharf (model *lf_gw_4* from Table 5).

Parameter	Parameter label	Mean	SD	2.5%	Median	97.5%
β_0	b_Intercept	-101.831	7.489	-118.103	-101.734	-84.935
β_d	b_date	0.052	0.004	0.043	0.052	0.062
μ_h	r_cohort[1,Intercept]	3.453	6.178	-13.278	1.214	28.413
μ_h	r_cohort[2,Intercept]	1.513	3.885	-11.108	0.606	16.960
μ_h	r_cohort[3,Intercept]	-0.660	3.423	-16.482	-0.101	12.577
μ_h	r_cohort[4,Intercept]	-1.604	3.770	-20.591	-0.571	11.827
μ_h	r_cohort[5,Intercept]	-0.725	4.753	-18.477	-0.236	18.895
σ^h	sd_cohort_Intercept	7.589	5.267	0.242	5.855	25.585
μ_d	r_cohort[1,date]	0.019	0.005	0.008	0.019	0.029
μ_d	r_cohort[2,date]	0.008	0.004	-0.001	0.008	0.016
μ_d	r_cohort[3,date]	0.000	0.004	-0.009	0.000	0.008
μ_d	r_cohort[4,date]	-0.005	0.004	-0.013	-0.005	0.004
μ_d	r_cohort[5,date]	-0.010	0.004	-0.019	-0.010	-0.002
σ^d	sd_cohort__date	0.016	0.006	0.006	0.014	0.038
–	cor_cohort__Intercept__date	0.059	0.732	-0.932	0.095	0.964
σ	sigma	0.517	0.356	0.017	0.399	1.831

Table C.9: Parameter estimates from model *tag9* (see Table 4) for estimating the growth rate of juvenile red rock lobster from mark-recapture size increment data collected at Halfmoon Bay, Stewart Island.

Parameter	Parameter label	Mean	SD	2.5%	Median	97.5%
β_0	b_Intercept	0.018	0.076	-0.135	0.019	0.163
β_s	b_sexMale	0.098	0.087	-0.065	0.097	0.263
–	bs_syears_lib_1	-0.481	0.050	-0.576	-0.481	-0.380
–	s_syears_lib_1[1]	-3.930	0.858	-5.677	-3.901	-2.322
–	sds_syears_lib_1	4.062	1.679	1.471	3.478	9.819
–	bs_scl_rel_1	0.216	0.047	0.121	0.215	0.310
–	s_scl_rel_1[1]	-1.387	0.948	-3.146	-1.377	0.110
–	sds_scl_rel_1	2.286	1.360	0.179	1.863	7.269

Table C.10: Parameter estimates from the selected model (Equation 7, Equation 8) for predicting the growth rate of post-settlement red rock lobsters from a tank-based captive lobster study at NIWA, Mahanga Bay, Wellington (*mah4* from Table 8). This table omits the parameters for the random slope and intercept for lobster ID, which are numerous.

Parameter	Parameter label	Mean	SD	2.5%	Median	97.5%
β_0	b_Intercept	13.236	0.226	12.784	13.235	13.705
β_d	b_days	0.057	0.002	0.054	0.057	0.060
–	sd_lob_id__Intercept	1.489	0.174	1.165	1.474	1.912
–	sd_lob_id__days	0.010	0.001	0.007	0.010	0.013
–	cor_lob_id__Intercept__days	0.114	0.180	-0.223	0.111	0.460
σ	sigma	1.116	0.045	1.031	1.116	1.207